Supporting Information

Coligand-Dependent Cellular Effects and DNA/BSA Binding of Ruthenium(II) Tris(Pyrazolylmethane) Complexes

Alberto Gobbo,[a] Ján Vančo,[b] Sara Benetti,[a] Tomáš Malina,[b,c] Zdeněk Dvořák,[d] Christian Castelli,[a] Alessio Chiappa,[a] Massimo Guelfi,[a] Stefano Zacchini,[e] Tarita Biver,[a,*] Zdeněk Trávníček,[b,*] Fabio Marchetti [a,*]

[a] Department of Chemistry and Industrial Chemistry, University of Pisa, Via G. Moruzzi 13, I-56124 Pisa, Italy

[b] Regional Centre of Advanced Technologies and Materials, Czech Advanced Technology and Research Institute, Palacký University, Šlechtitelů 27, CZ-779 00 Olomouc, Czech Republic

[c] Nanotechnology Centre, Centre for Energy and Environmental Technologies, VŠB–Technical University of Ostrava, 17. listopadu 2172/15, CZ-708 00 Ostrava-Poruba, Czech Republic

[d] Department of Cell Biology and Genetics, Faculty of Science, Palacký University, Šlechtitelů 27, CZ-779 00 Olomouc, Czech Republic

[e] Department of Industrial Chemistry "Toso Montanari", University of Bologna, Viale Risorgimento 4, I-40136 Bologna, Italy

[f] Center for Instrument Sharing of the University of Pisa (CISUP), Lungarno Pacinotti, 43/44, I-56126 Pisa, Italy

*E-mail addresses: tarita.biver@unipi.it; zdenek.travnicek@upol.cz; fabio.marchetti@unipi.it

Table of contents **Pages**

Table S1. Hydrogen bonds for **4·H₂O** [Å and °].

D-H···A	d(D-H)	d(H···A)	d(D···A)	<(DHA)
O(1)-H(1) ··Cl(2)	0.990	2.234	3.135(2)	150.81
O(1)-H(6) ··Cl(2)#1	0.985	2.226	3.203(2)	171.20

Symmetry transformations used to generate equivalent atoms: #1 -x, -y, -z.

Table S2. Hydrogen bonds for **5**·0.331Et_2O·0.169CH_2Cl_2·H_2O [Å and °].

D-H···A	d(D-H)	d(H···A)	d(D···A)	<(DHA)
O(1)-H(251)···Cl(2)#1	0.84(2)	2.40(2)	3.161(10)	152(6)
O(1)-H(205)···Cl(2)#2	0.851(19)	2.409(19)	3.224(10)	161(7)

Symmetry transformations used to generate equivalent atoms: #1 -x+2, -y+1, -z+1; #2 x, y, z+1.

Table S3. Hydrogen bonds for **6**·0.5CH_2Cl_2 [Å and °].

D-H···A	d(D-H)	d(H···A)	d(D···A)	<(DHA)
N(7)-H(7A)···Cl(2)#1	0.91	2.52	3.302(3)	144.8
O(1)-H(1A)···Cl(1)#2	0.84	2.41	3.247(3)	177.8

Symmetry transformations used to generate equivalent atoms: #1 x+1/2, -y+3/2, z+1/2; #2 x-1/2, -y+3/2, z-1/2.

Table S4. Hydrogen bonds for **7** [Å and °].

D-H···A	d(D-H)	d(H···A)	d(D···A)	<(DHA)
O(1)-H(1) ··Cl(2)	0.84	2.20	3.007(2)	161.0

Table S5. Selected bond lengths (Å) and angles (°) for complexes **4**, **5** and **6**

4		**5**		**6**	
Ru1-N1	2.143(3)	Ru1-N1	2.082(9)	Ru1-N1	2.124(3)
Ru1-N3	2.080(3)	Ru1-N3	2.127(9)	Ru1-N3	2.055(3)
Ru1-N5	2.159(3)	Ru1-N5	2.061(9)	Ru1-N5	2.076(3)
Ru1-P1	2.3385(11)	Ru1-N7	2.073(9)	Ru1-N7	2.141(3)
Ru1-P2	2.2613(11)	Ru1-P1	2.327(3)	Ru1-P1	2.3062(8)
Ru1-Cl1	2.4124(10)	Ru1-Cl1	2.410(3)	Ru1-Cl1	2.4080(8)
N1-Ru1_N3	83.95(13)	N1-Ru1-N3	85.0(3)	N1-Ru1-N3	84.82(10)
N1-Ru1-N5	82.78(13)	N1-Ru1-N5	87.6(4)	N1-Ru1-N5	84.51(10)
N3-Ru1-N5	86.75(13)	N3-Ru1-N5	85.8(3)	N3-Ru1-N5	88.20(11)
P1-Ru1-P2	91.19(4)	P1-Ru1-N7	94.0(3)	P1-Ru1-N7	95.23(7)
P1-Ru1-Cl1	97.00(3)	P1-Ru1-Cl1	97.11(10)	P1-Ru1-Cl1	96.20(3)
P2-Ru1-Cl1	83.30(4)	N7-Ru1-Cl1	89.0(3)	N7-Ru1-Cl1	87.25(7)

Table S6. Selected bond lengths (Å) and angles (°) for complexes **7** and **14**

7		**14**	
Ru1-N1	2.0541(18)	Ru1-N1	2.120(3)
Ru1-N3	2.1421(19)	Ru1-N3	2.058(4)
Ru1-N5	2.0694(18)	Ru1-N5	2.054(4)
Ru1-N7	2.1423(19)	Ru1-N7	2.023(4)
Ru1-P1	2.2933(6)	Ru1-N8	2.022(4)
Ru1-Cl1	2.4081(6)	Ru1-P1	2.3337(11)
N1-Ru1-N3	81.56(7)	N7-C15	1.146(6)
N1-Ru1-N5	89.31(7)	N8-C13	1.130(6)
N3-Ru1-N5	83.84(7)	N1-Ru1-N3	83.72(14)
P1-Ru1-N7	92.95(5)	N1-Ru1-N5	83.29(14)
P1-Ru1-Cl1	98.44(2)	N3-Ru1-N5	89.18(15)
N7-Ru1-Cl1	83.76(6)	P1-Ru1-N7	96.77(11)
		P1-Ru1-N8	95.12(11)
		N7-Ru1-N8	90.87(16)
		Ru1-N7-C15	165.2(4)
		Ru1-N8-C13	177.8(4)

IR spectra

Figure S1. Solid-state IR spectrum (650-4000 cm^{-1}) of **3**.

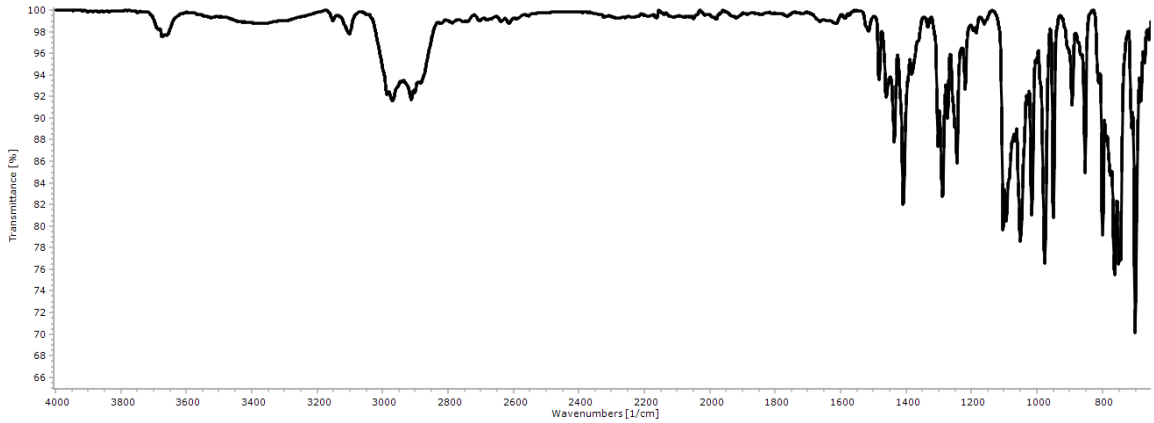

Figure S2. Solid-state IR spectrum (650-4000 cm^{-1}) of **4**.

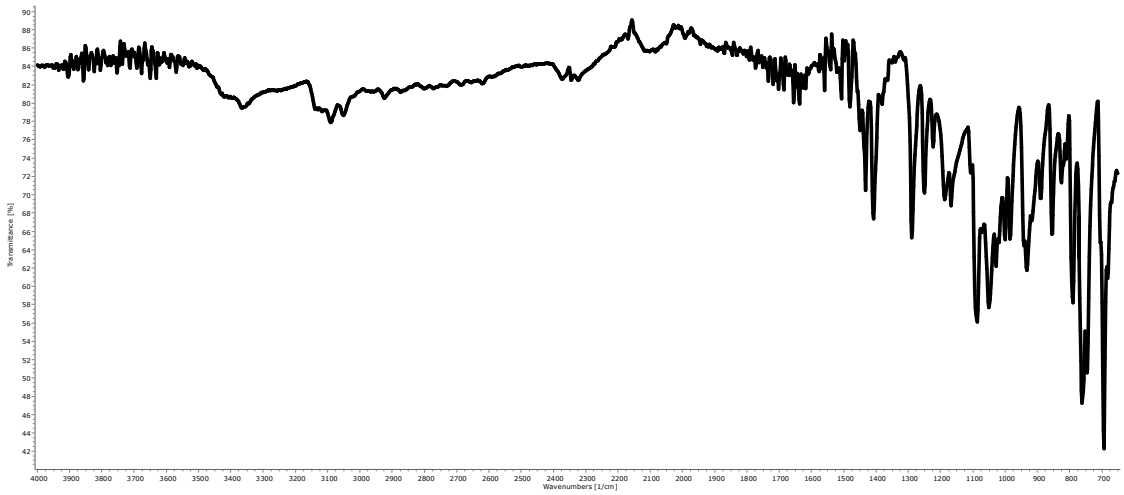

Figure S3. Solid-state IR spectrum (650-4000 cm^{-1}) of **5.**

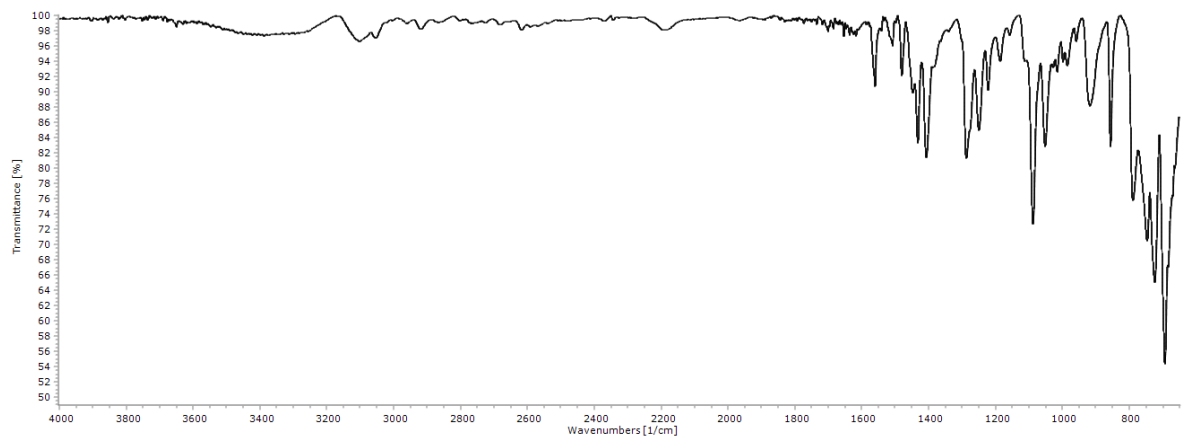

Figure S4. Solid-state IR spectrum (650-4000 cm^{-1}) of **6.**

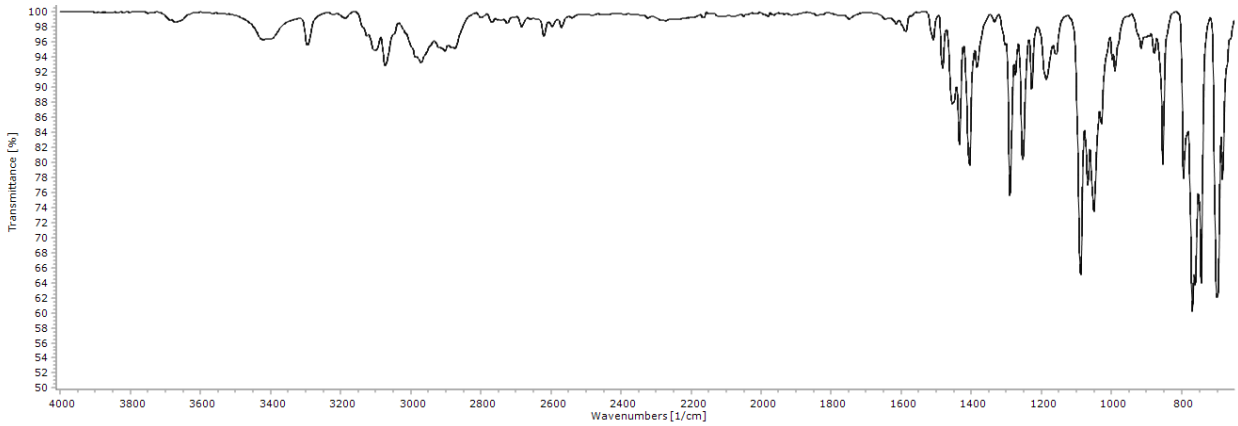

Figure S5. Solid-state IR spectrum (650-4000 cm^{-1}) of **7.**

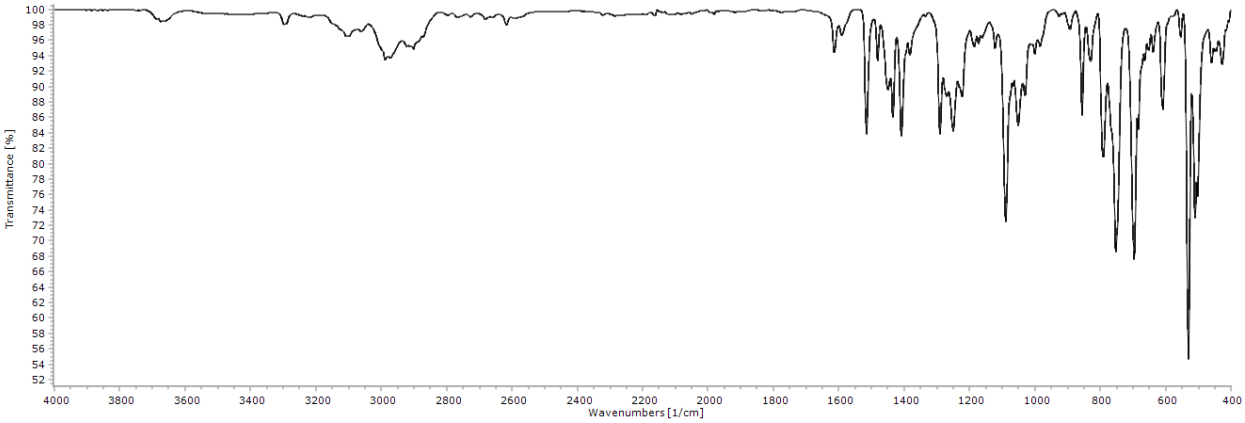

Figure S6. Solid-state IR spectrum (650-4000 cm^{-1}) of **8.**

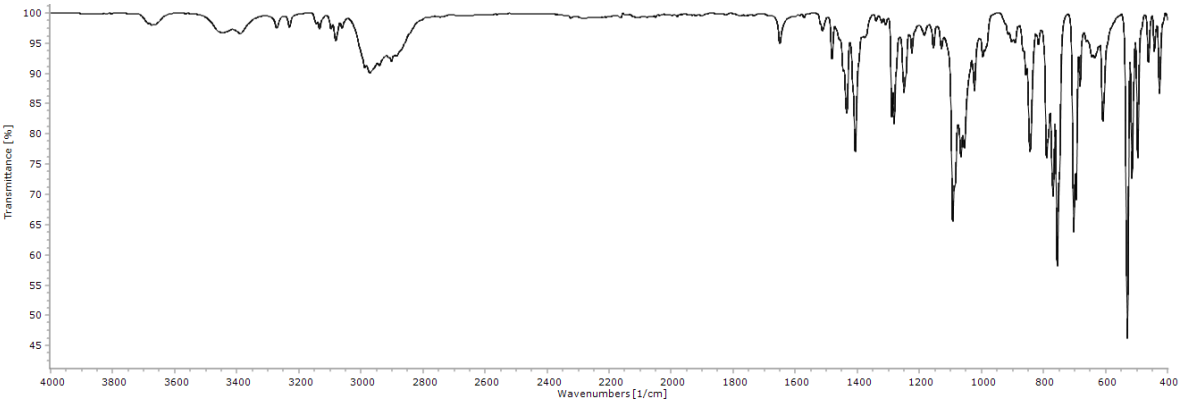

Figure S7. Solid-state IR spectrum (650-4000 cm^{-1}) of **9.**

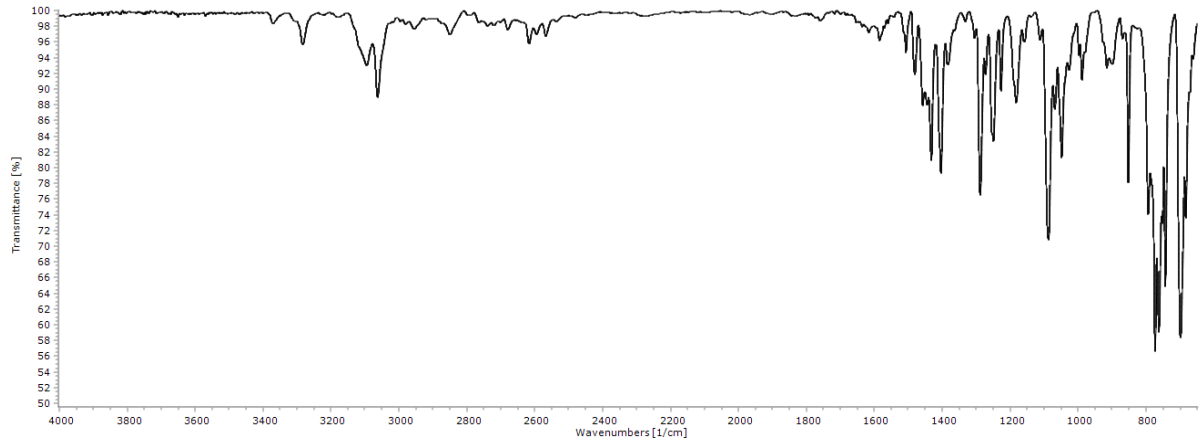

Figure S8. Solid-state IR spectrum (650-4000 cm^{-1}) of **13.**

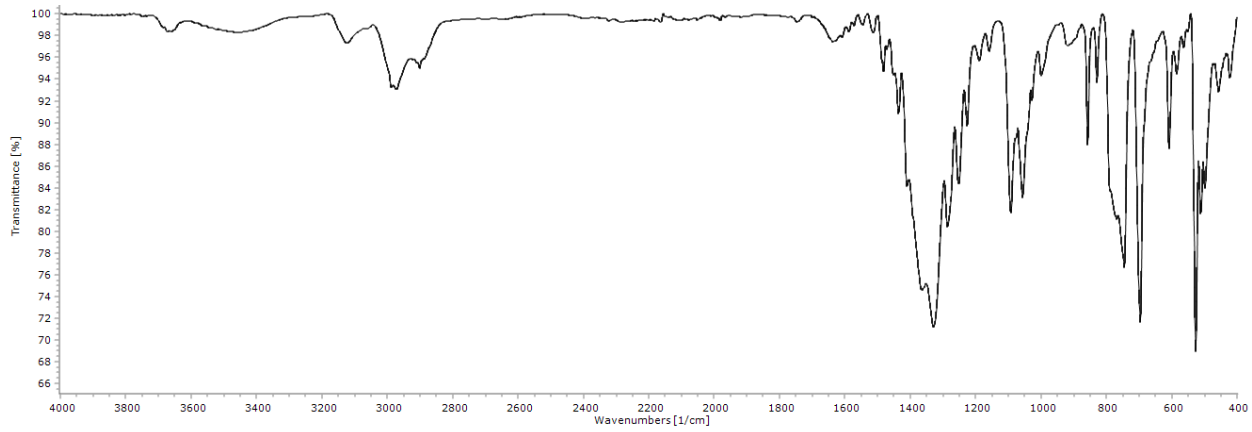

Figure S9. Solid-state IR spectrum (650-4000 cm^{-1}) of **14.**

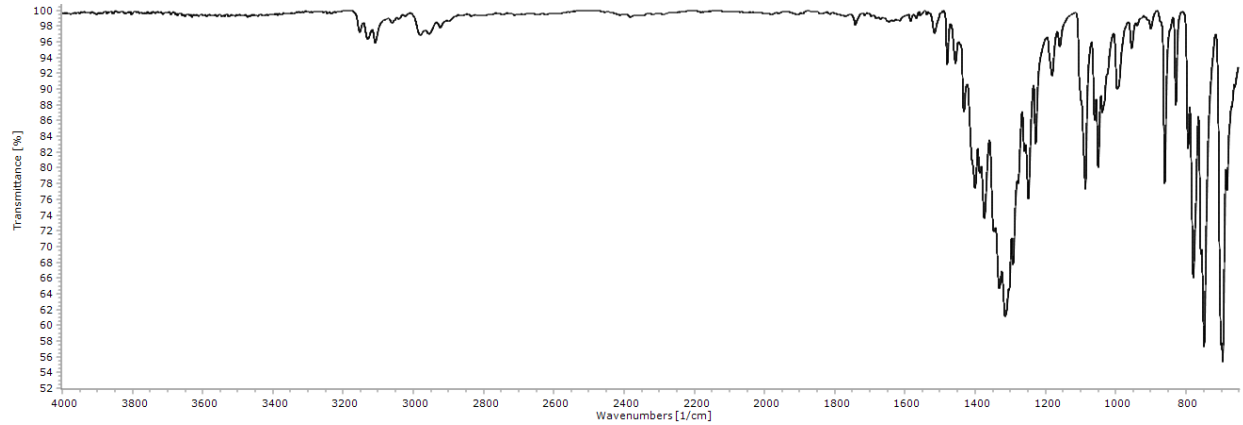

NMR spectra

Figure S10. ^{1}H NMR spectrum (401 MHz, CD_2Cl_2) of **3**.

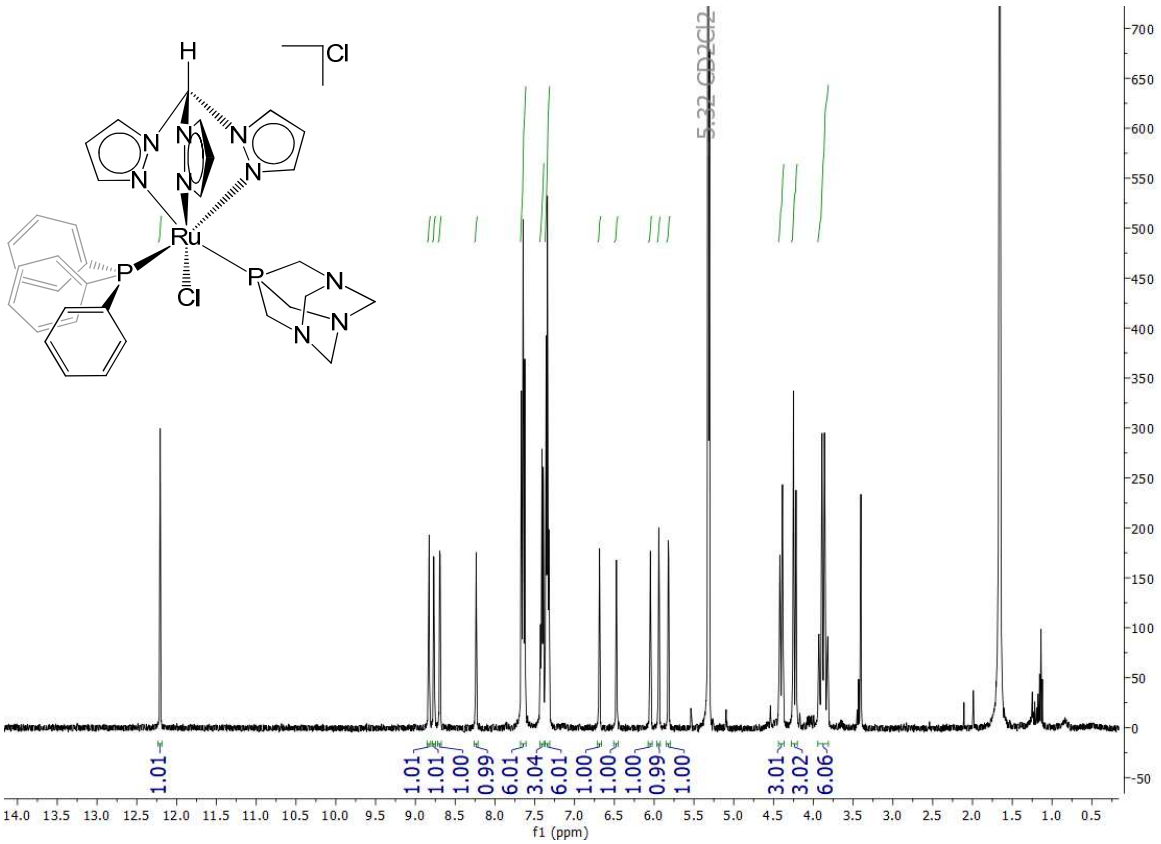

Figure S11. ^{31}P NMR spectrum (162 MHz, CD_2Cl_2) of **3**.

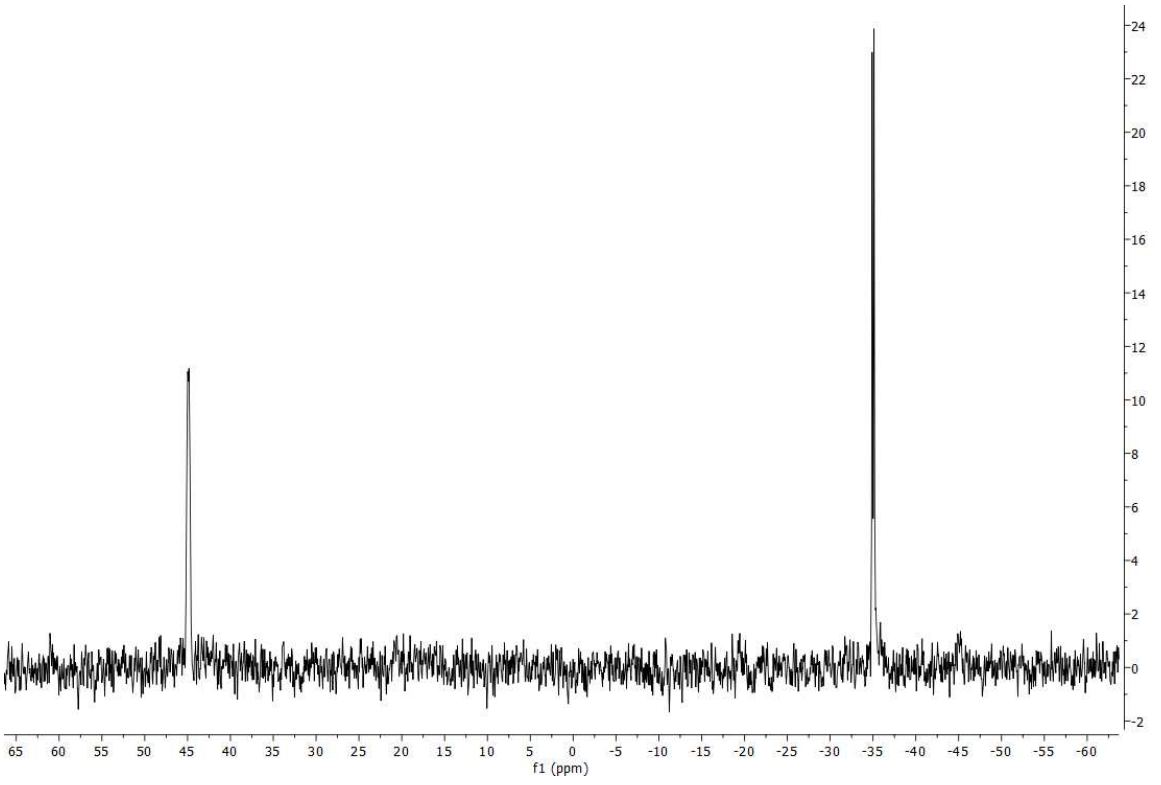

Figure S12. ^{1}H NMR spectrum (401 MHz, $CDCl_3$) of **4**.

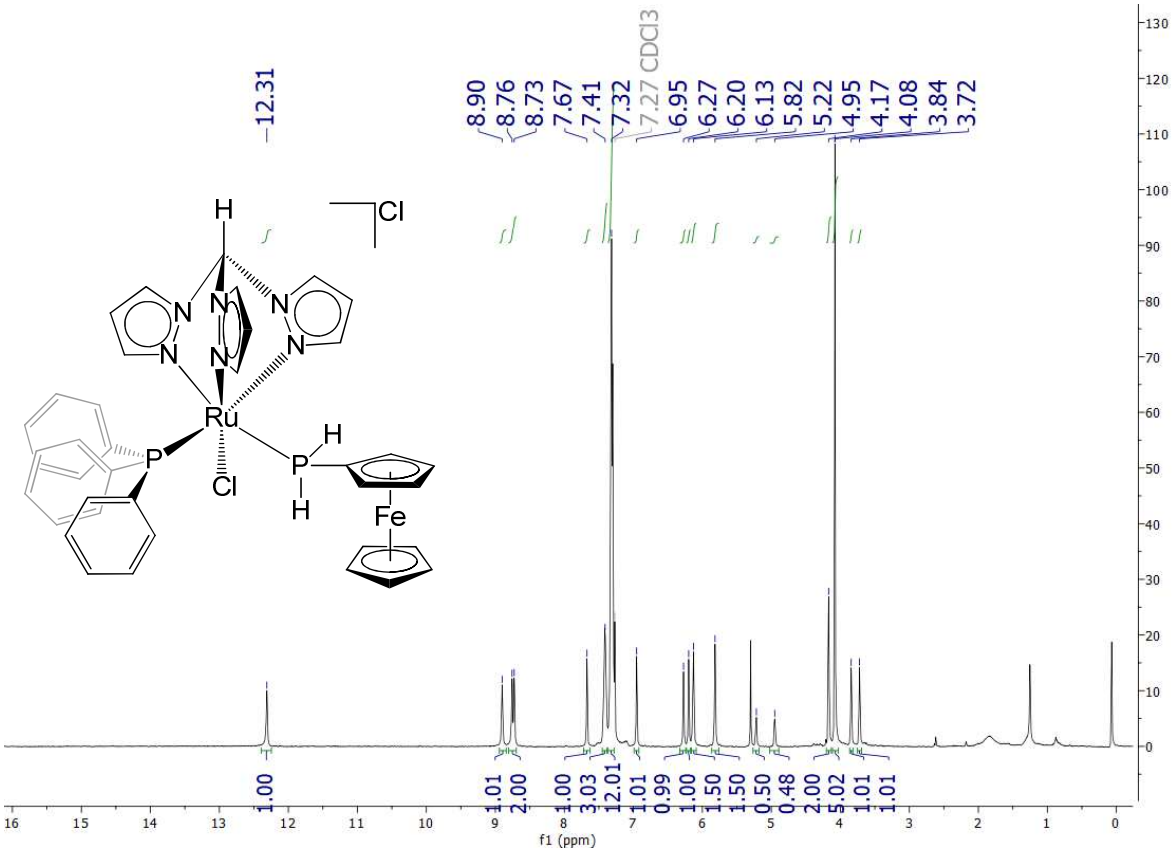

Figure S13. $^{13}C\{^{1}H\}$ NMR spectrum (101 MHz, $CDCl_3$) of **4**.

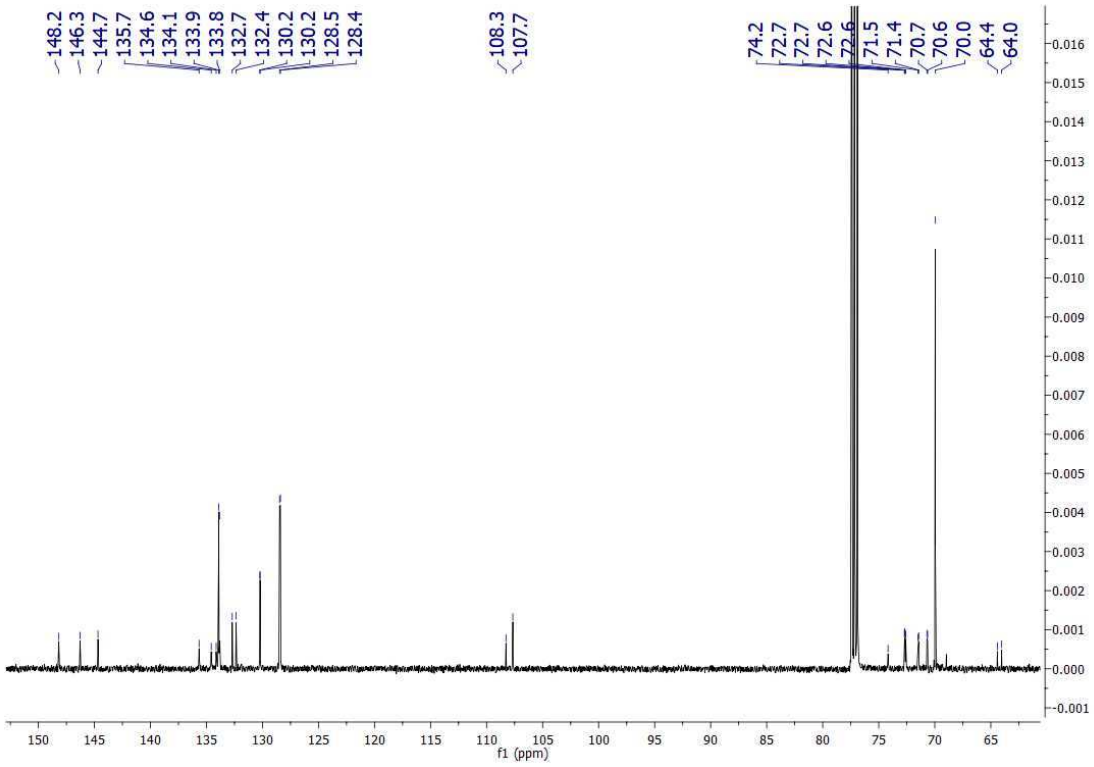

Figure S14. ^{31}P NMR spectrum (162 MHz, $CDCl_3$) of **4**.

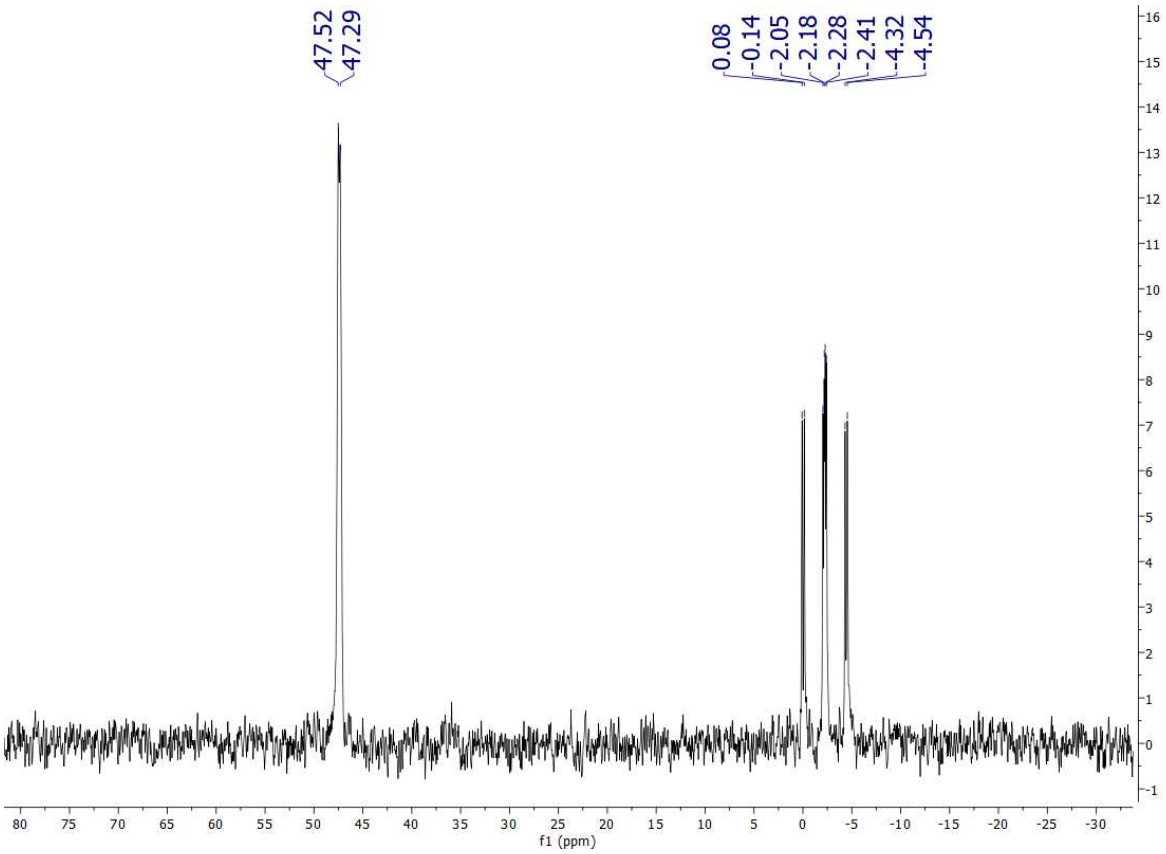

Figure S15. ^{1}H NMR spectrum (401 MHz, $CDCl_3$) of **5**.

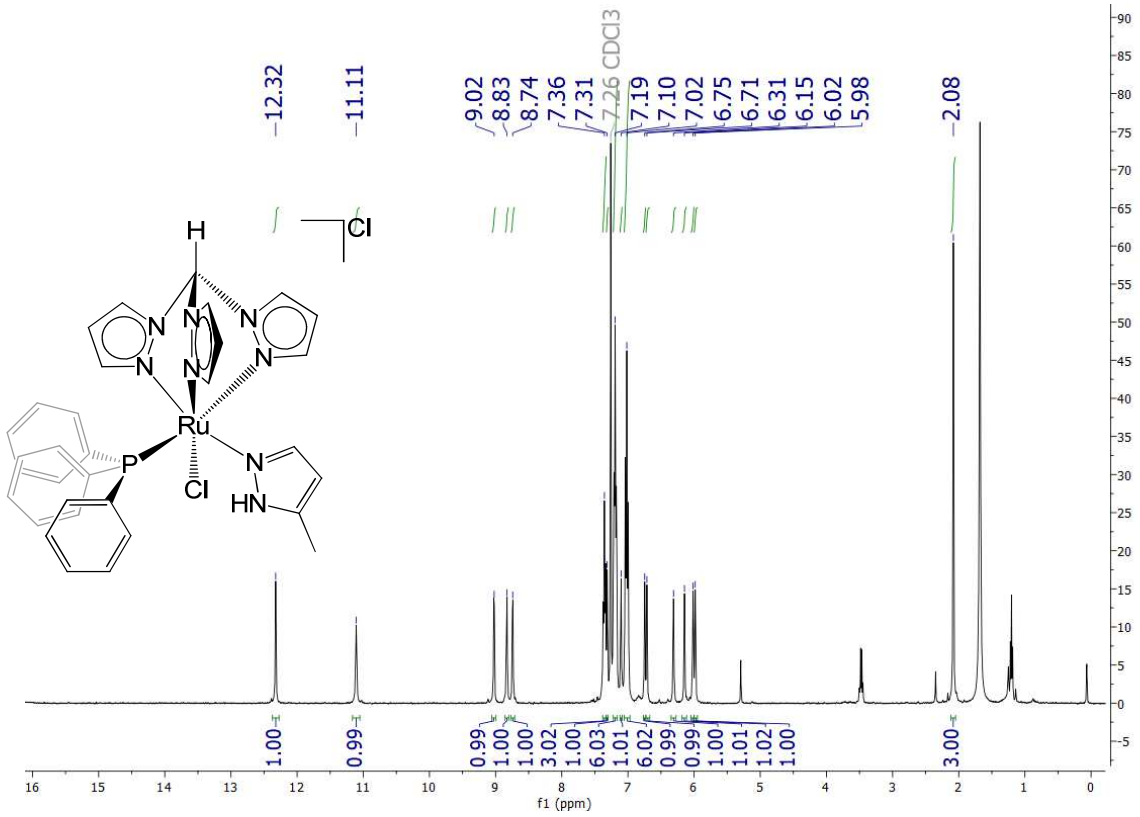

Figure S16. $^{13}C\{^{1}H\}$ NMR spectrum (101 MHz, $CDCl_3$) of **5**.

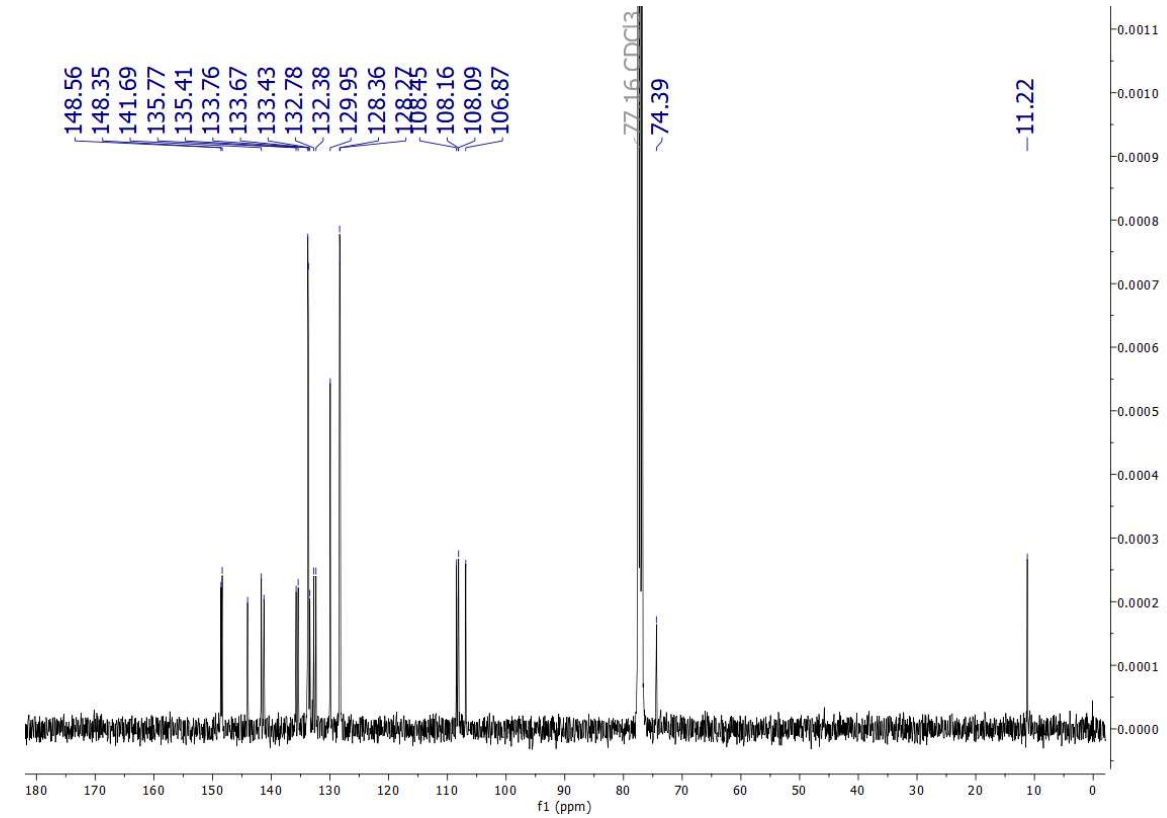

Figure S17. ^{31}P NMR spectrum (162 MHz, $CDCl_3$) of **5**.

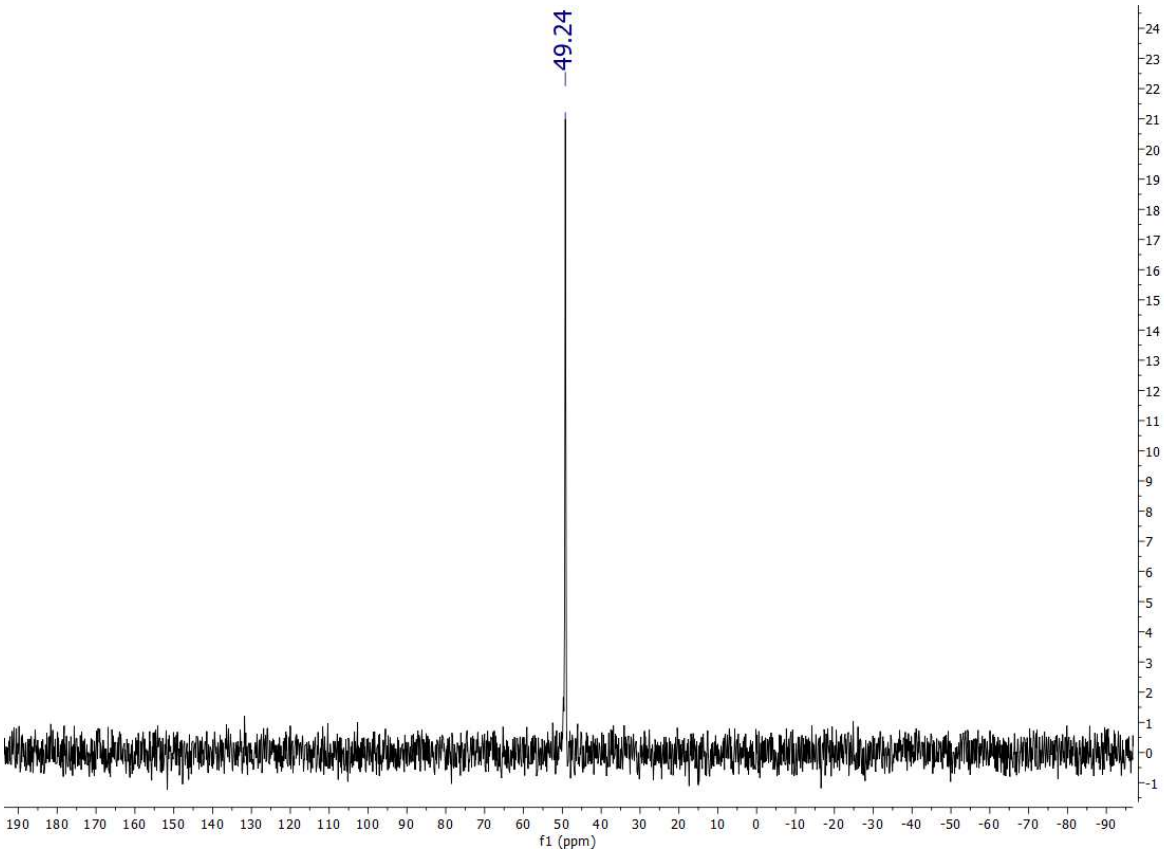

Figure S18. ^{1}H NMR spectrum (401 MHz, CD_3OD) of **6.**

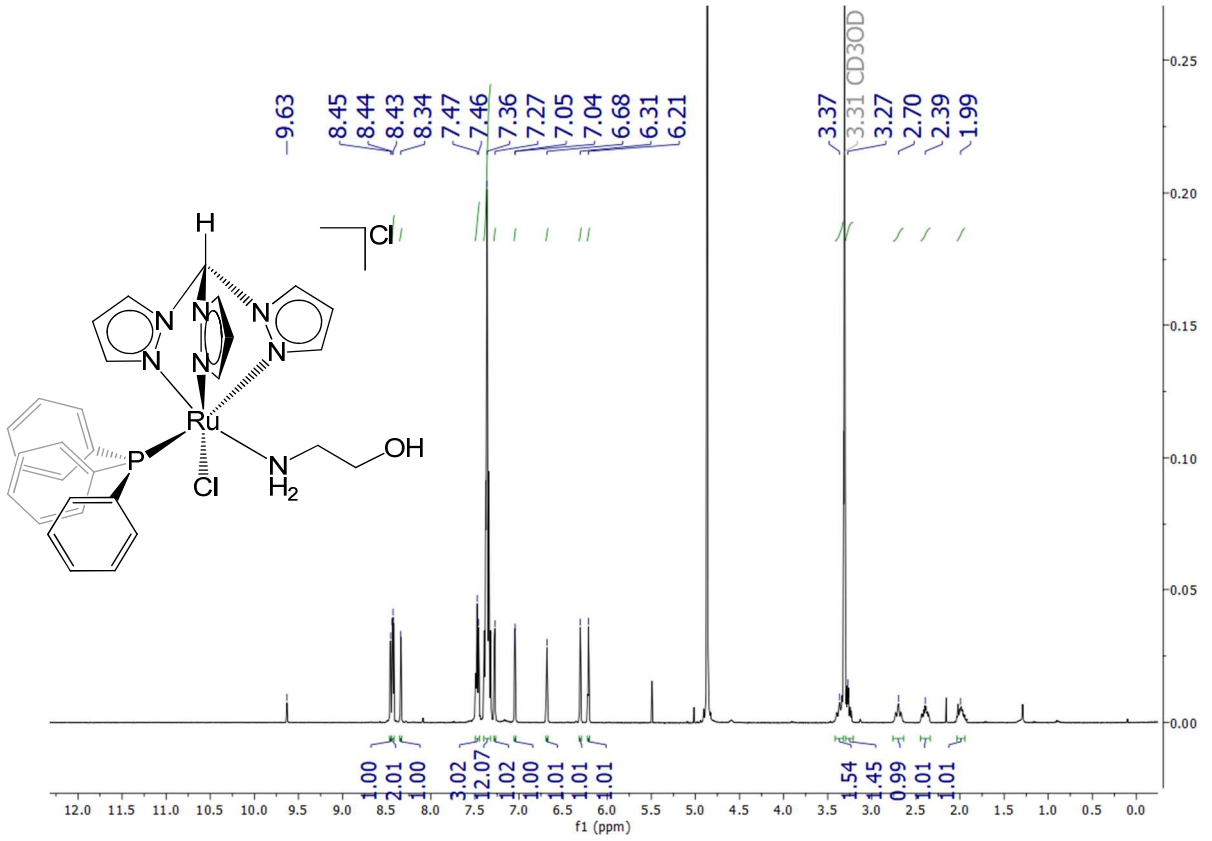

Figure S19. $^{13}C\{^{1}H\}$ NMR spectrum (101 MHz, CD_3OD) of **6.**

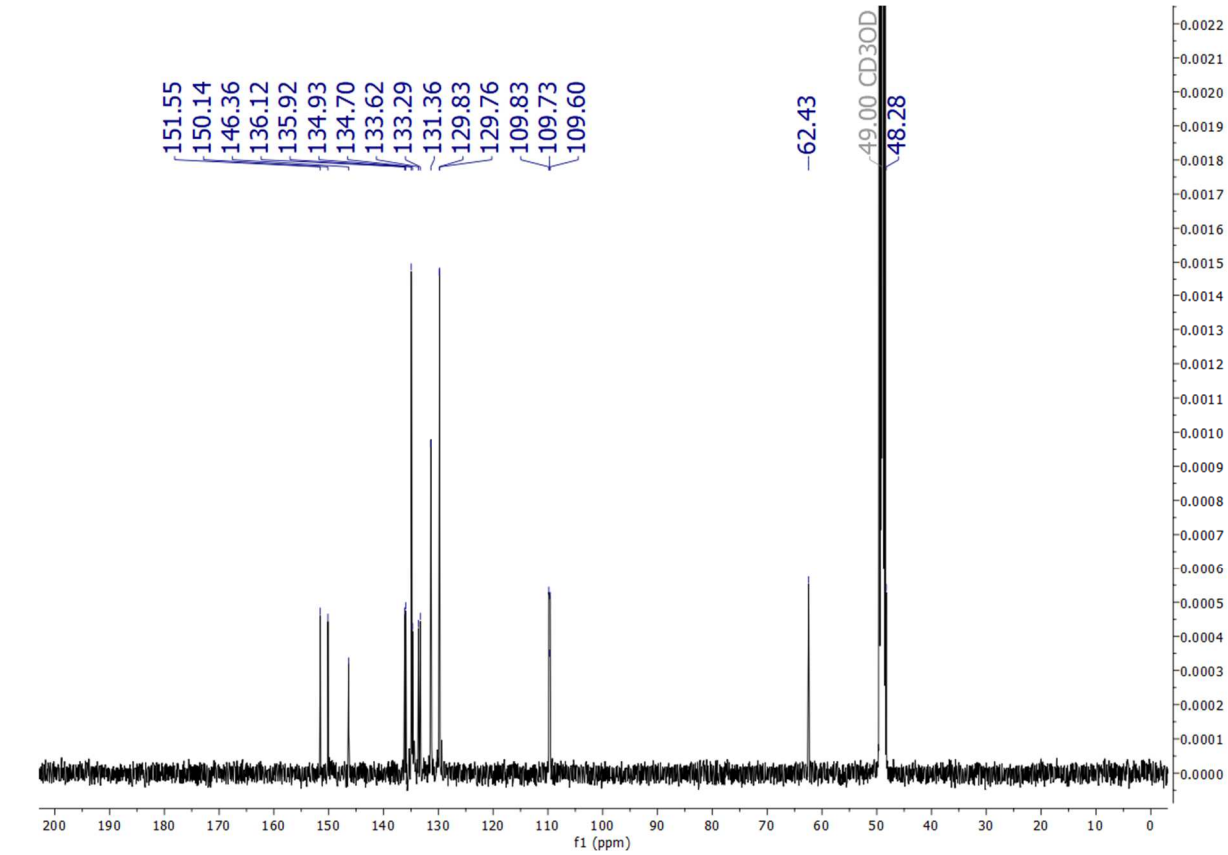

Figure S20. ^{31}P NMR spectrum (162 MHz, CD_3OD) of **6.**

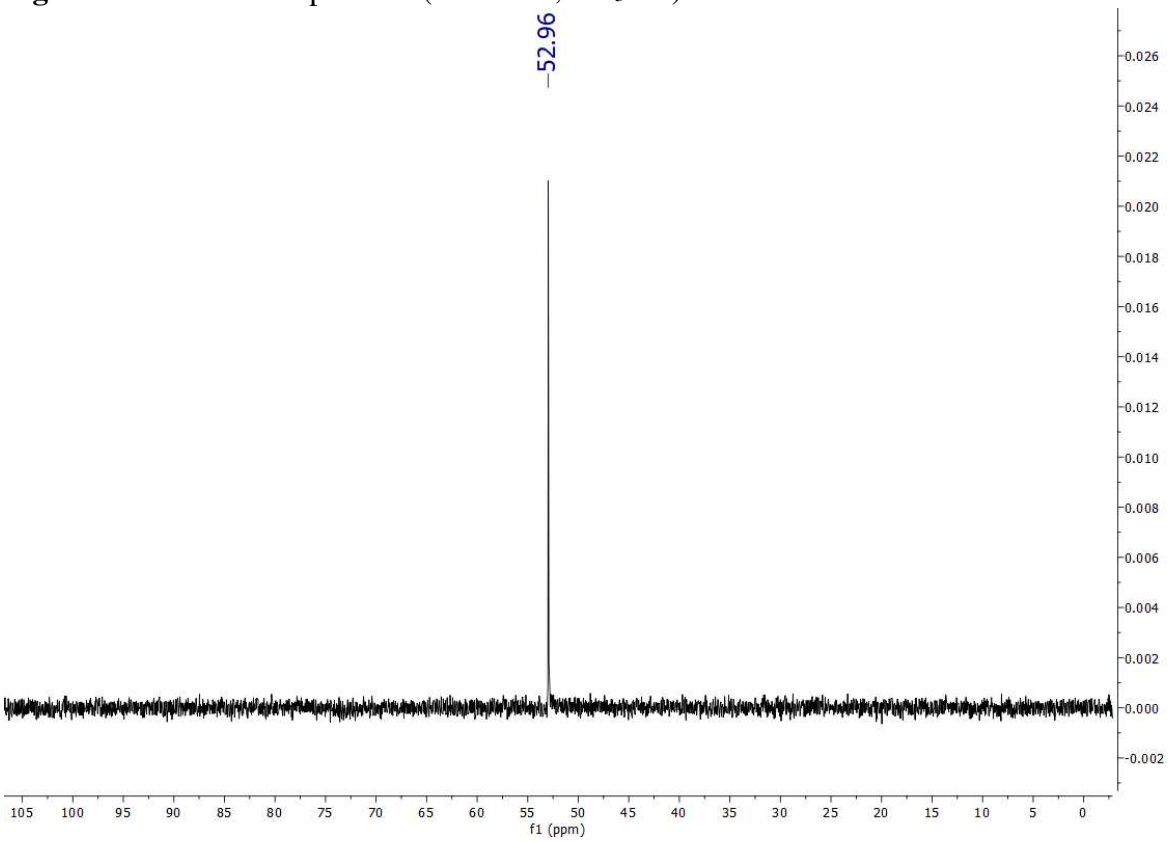

Figure S21. ^{1}H NMR spectrum (401 MHz, $CDCl_3$) of **7**.

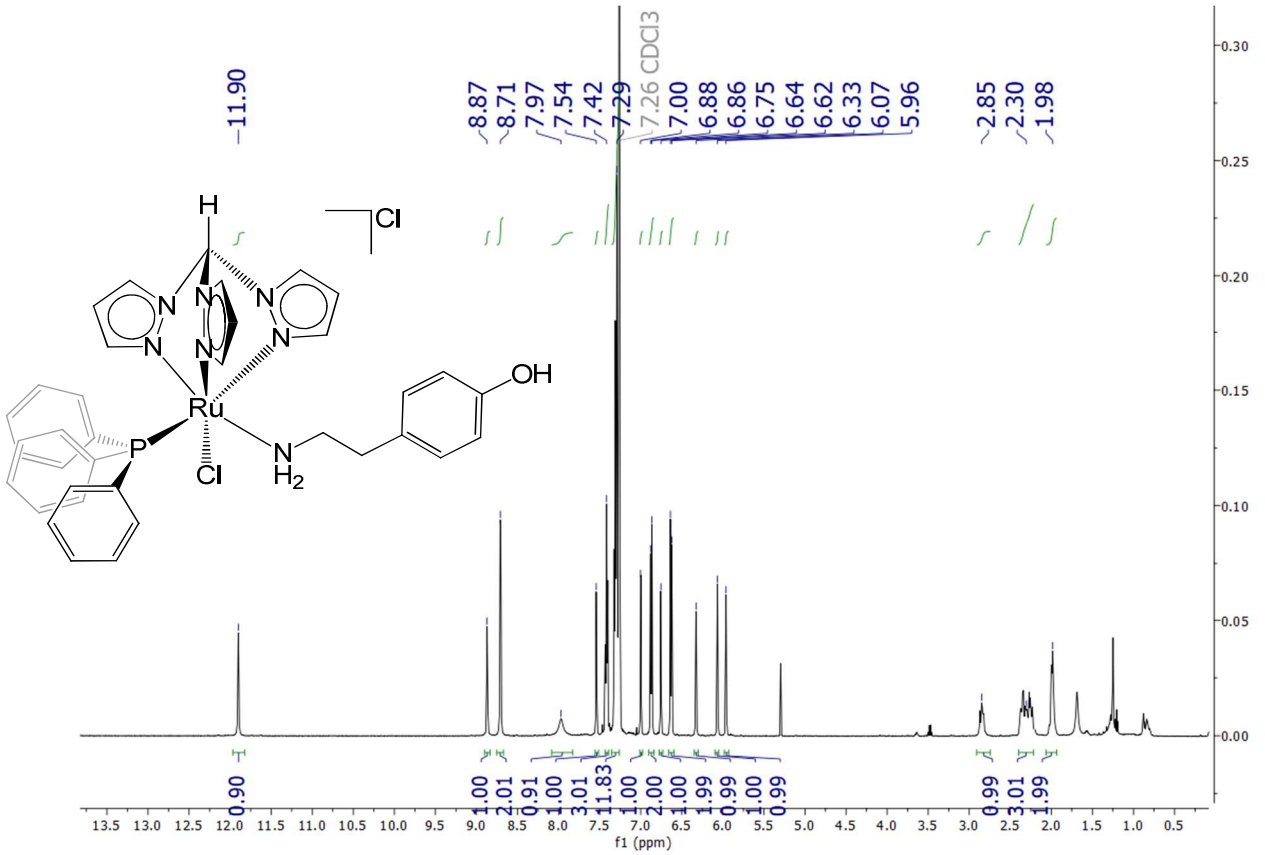

Figure S22. $^{13}C\{^{1}H\}$ NMR spectrum (101 MHz, $CDCl_3$) of **7.**

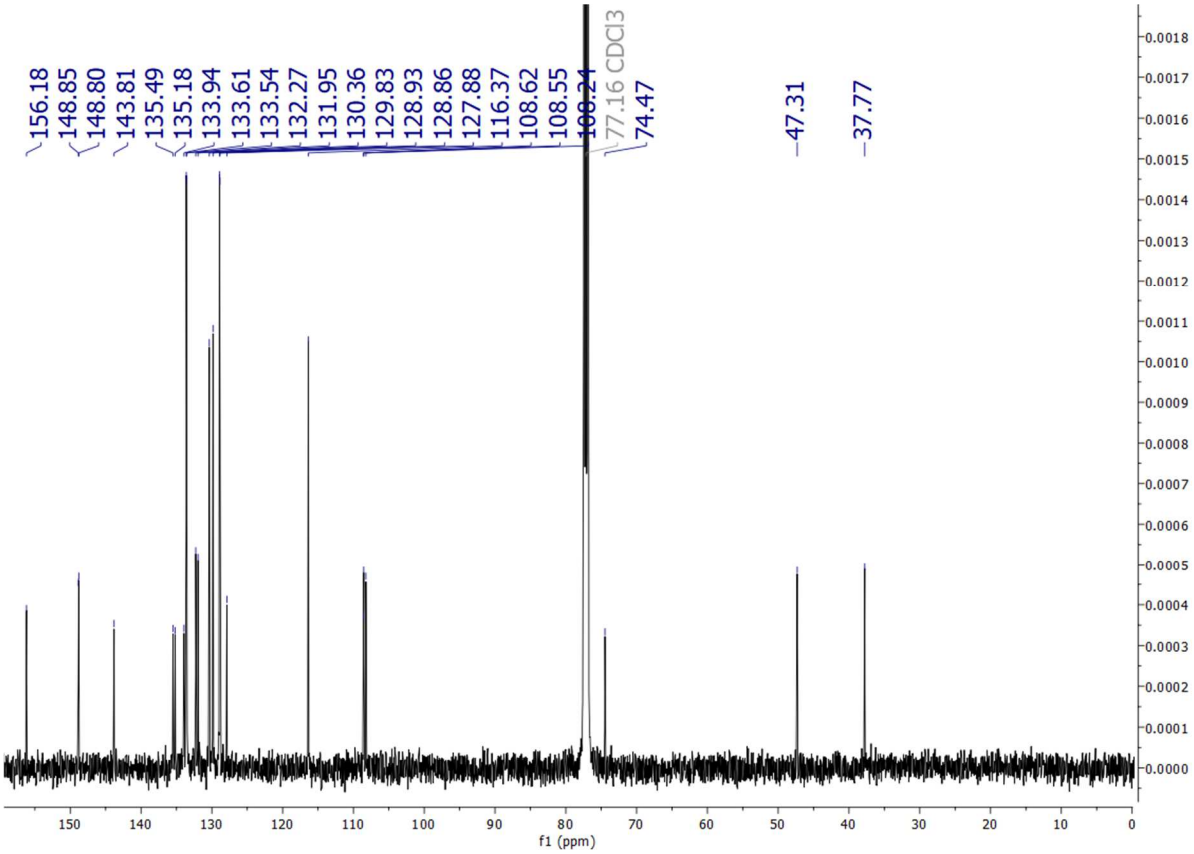

Figure S23. ^{31}P NMR spectrum (162 MHz, $CDCl_3$) of **7**.

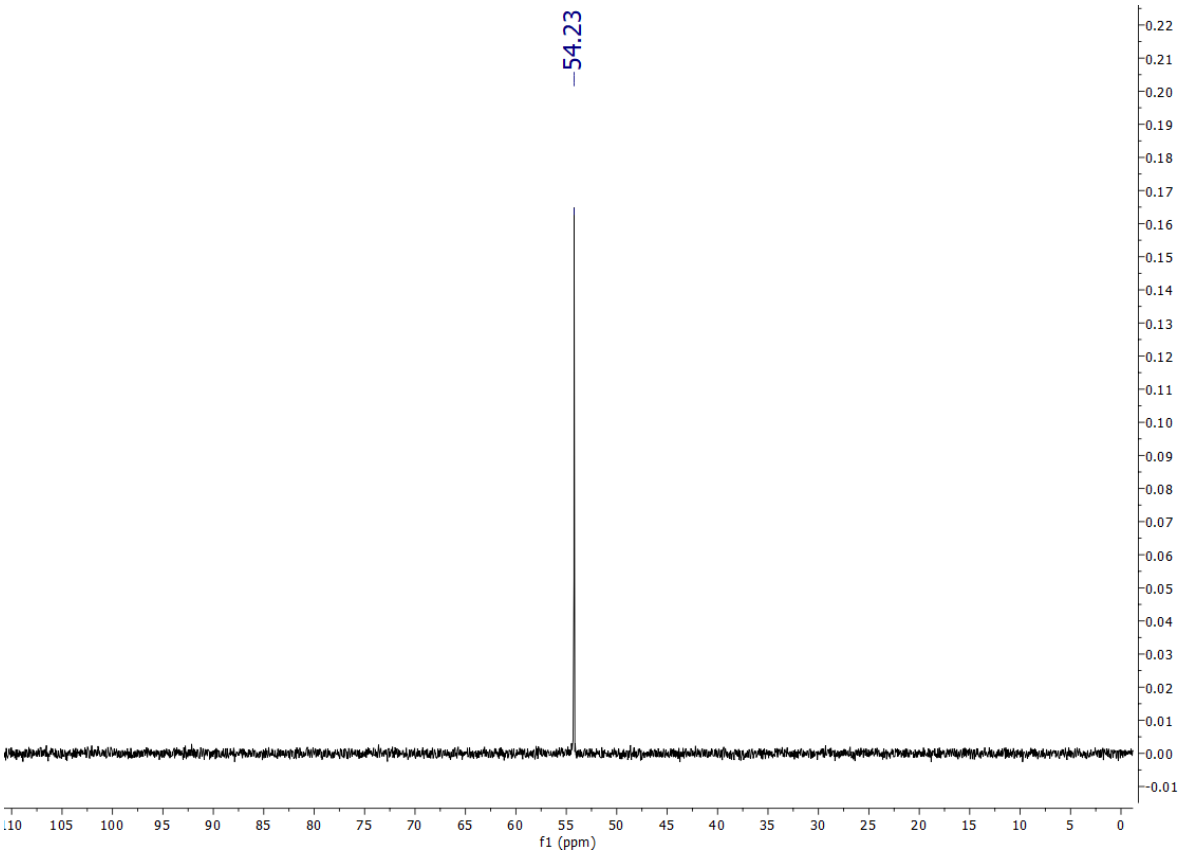

Figure S24. ^{1}H NMR spectrum (401 MHz, CD_3OD) of **8**.

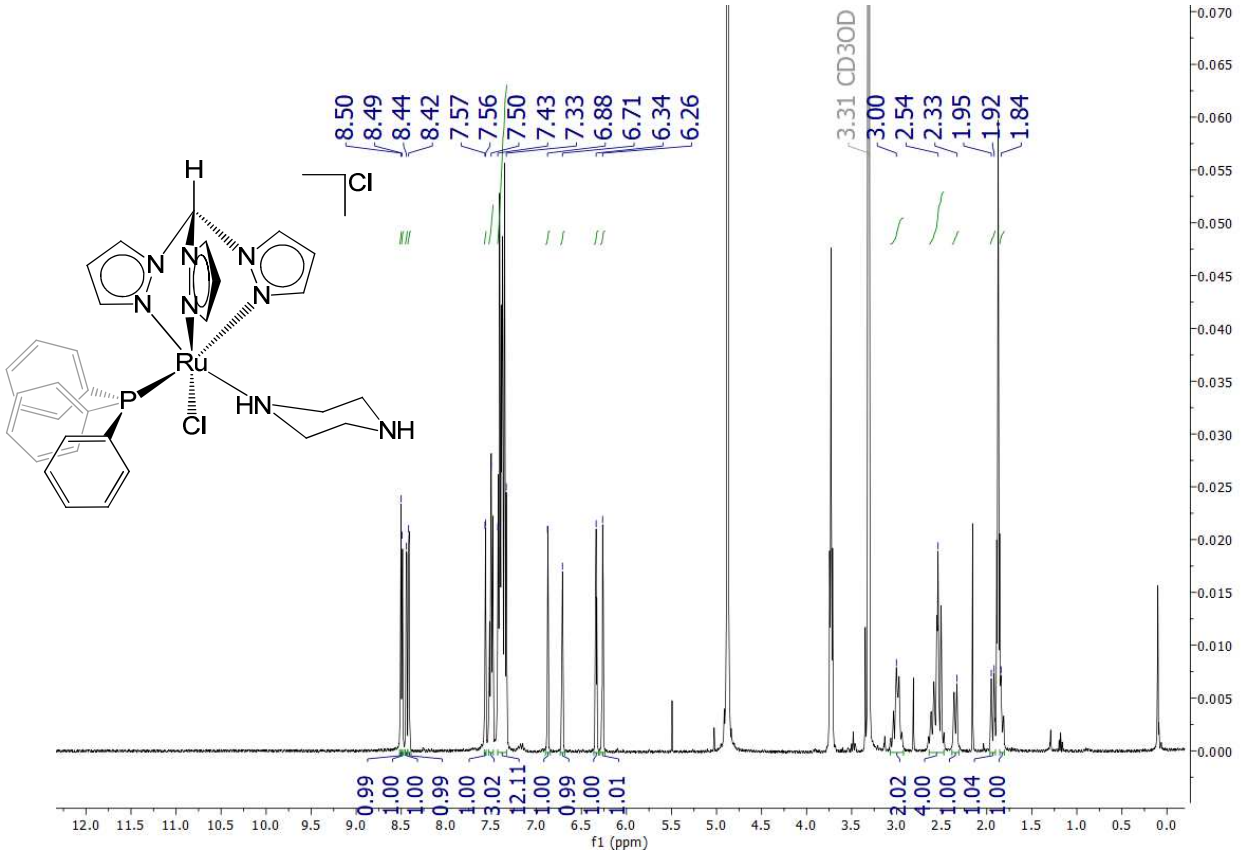

Figure S25. $^{13}C\{^{1}H\}$ NMR spectrum (101 MHz, CD_3OD) of **8.**

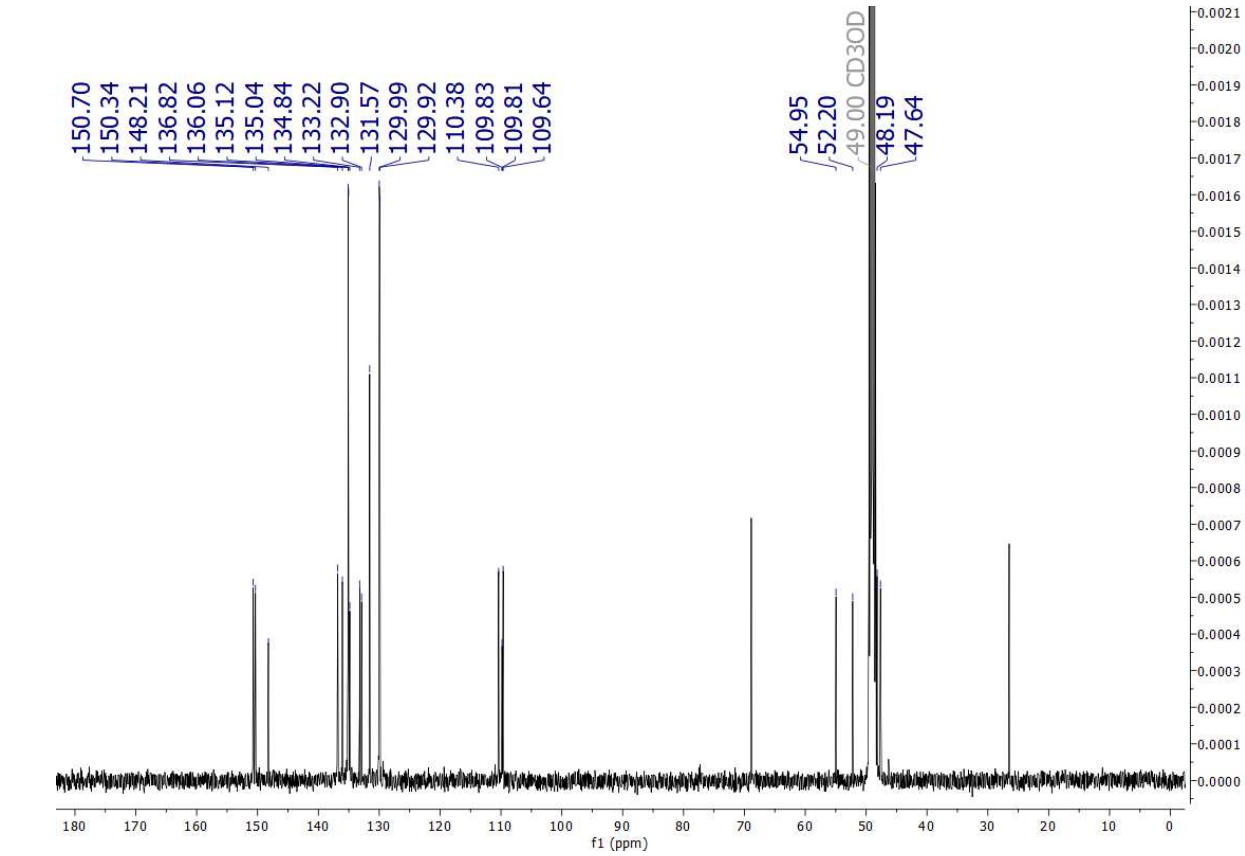

Figure S26. ^{31}P NMR spectrum (162 MHz, CD_3OD) of **8**.

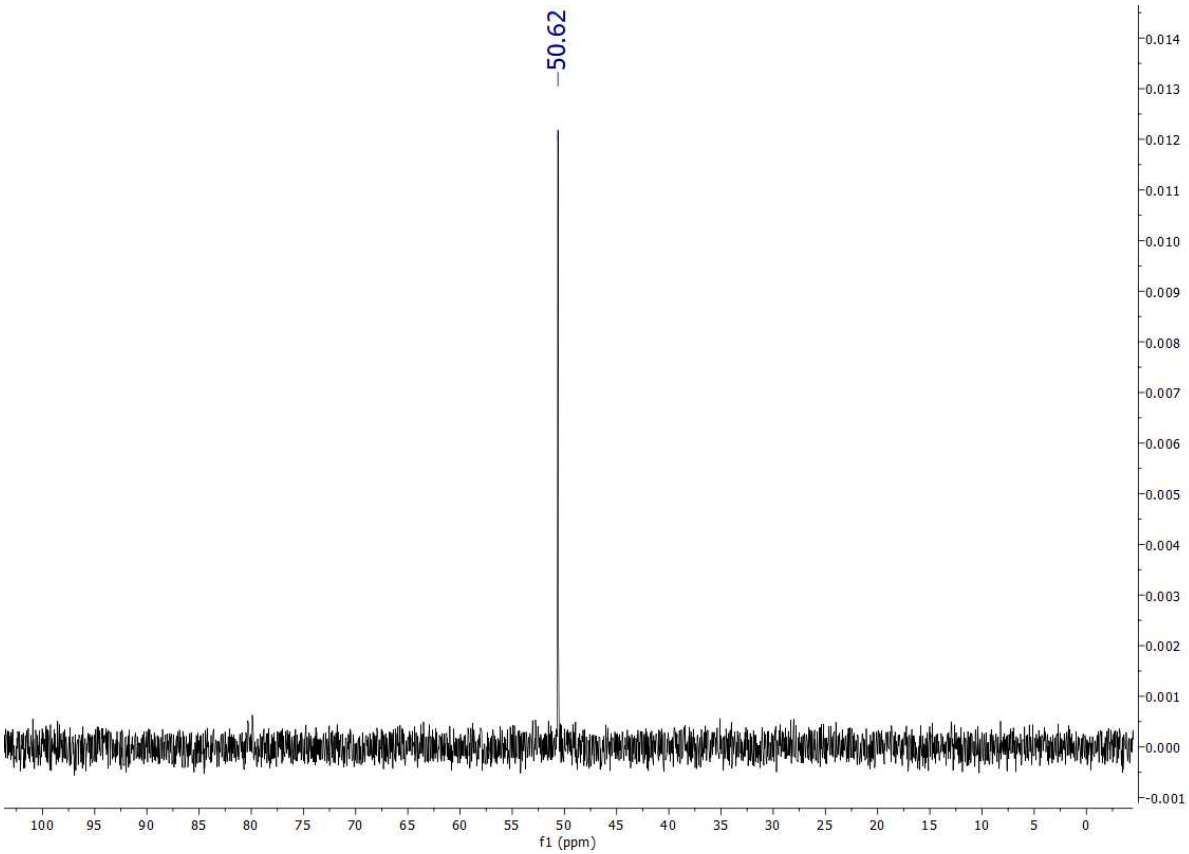

Figure S27. ^{1}H NMR spectrum (401 MHz, CD_3OD) of **9.**

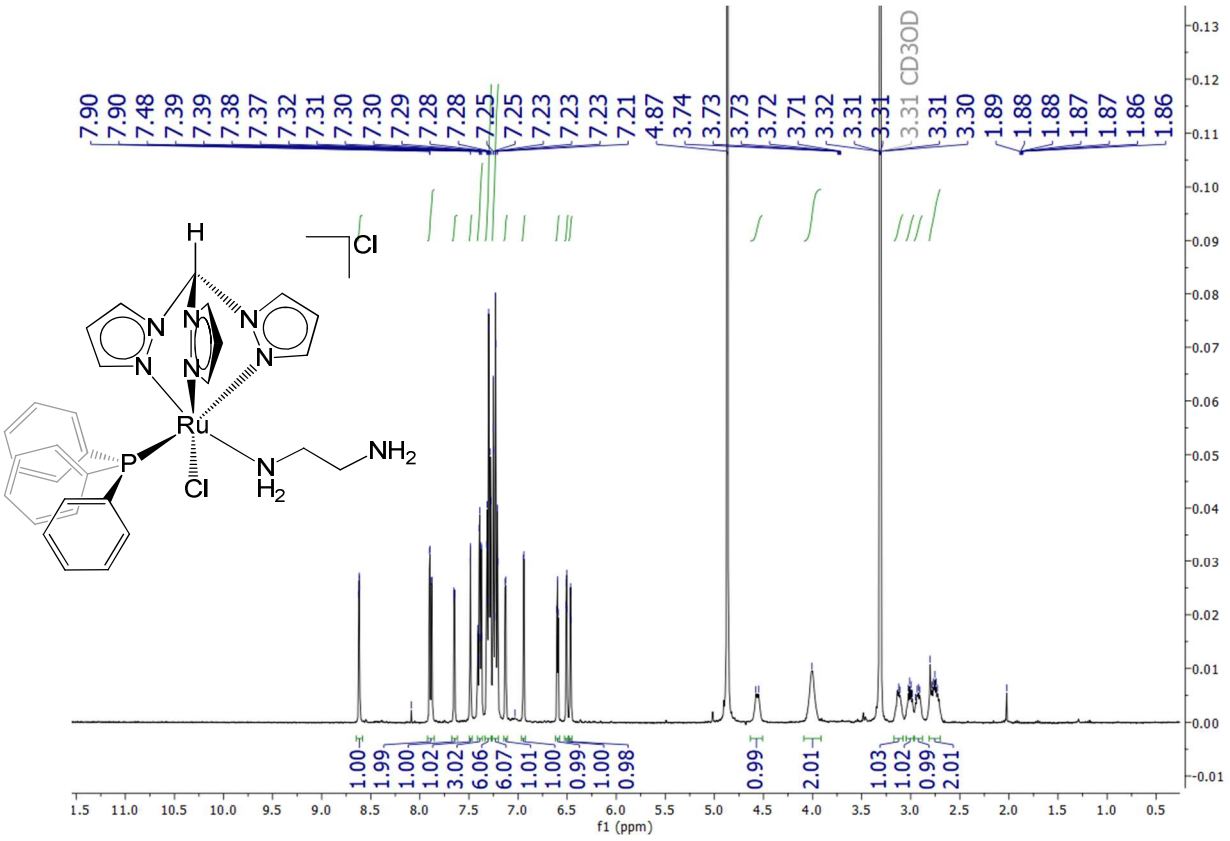

Figure S28. $^{13}C\{^{1}H\}$ NMR spectrum (101 MHz, CD_3OD) of **9.**

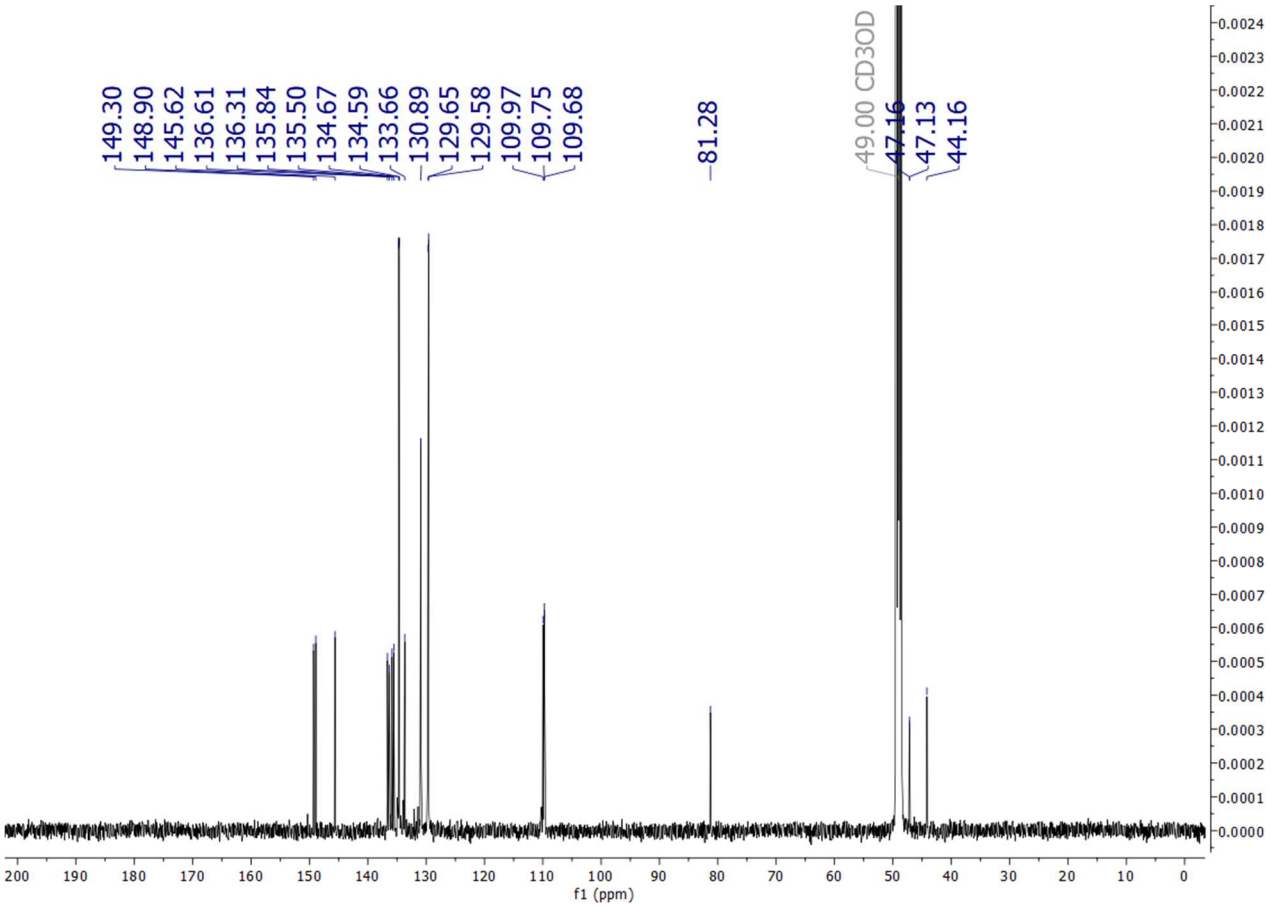

Figure S29. ^{31}P NMR spectrum (162 MHz, CD_3OD) of **9.**

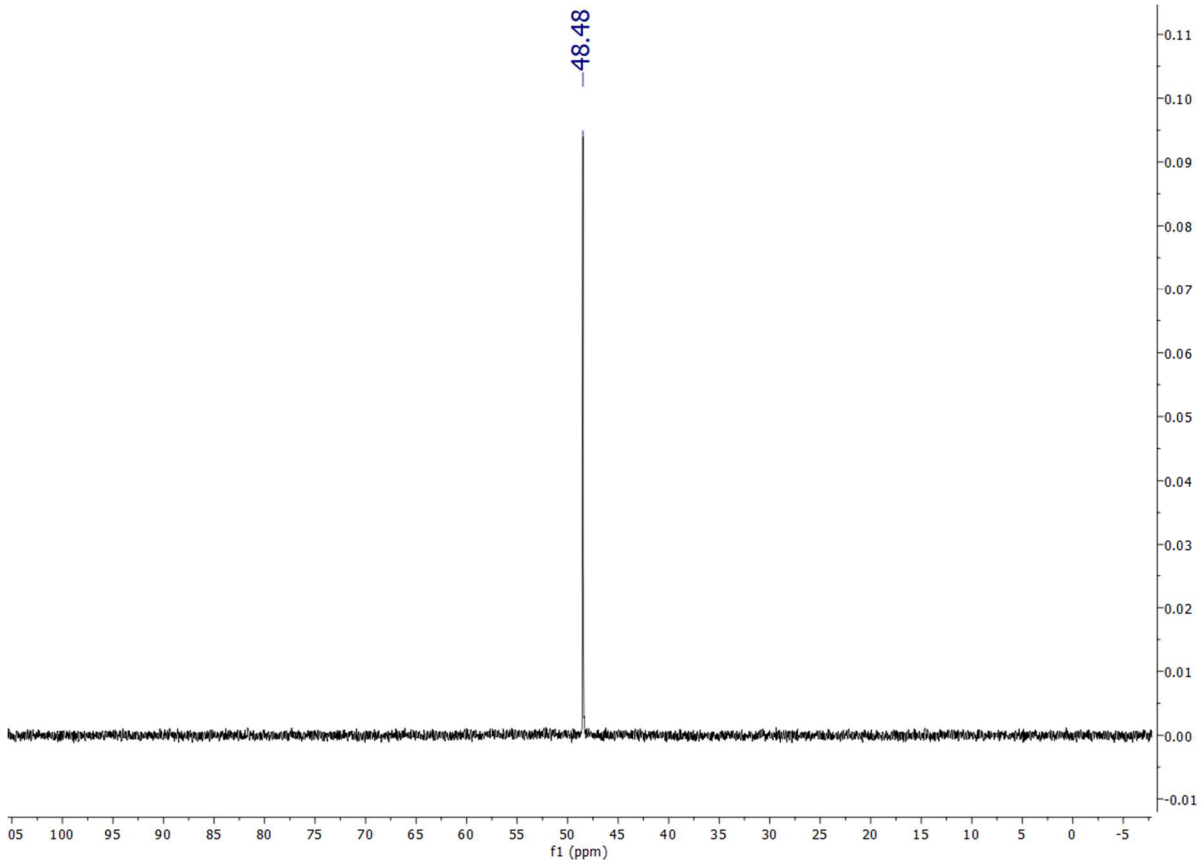

Figure S30. ^{1}H NMR spectrum (401 MHz, CD_3OD) of **13**

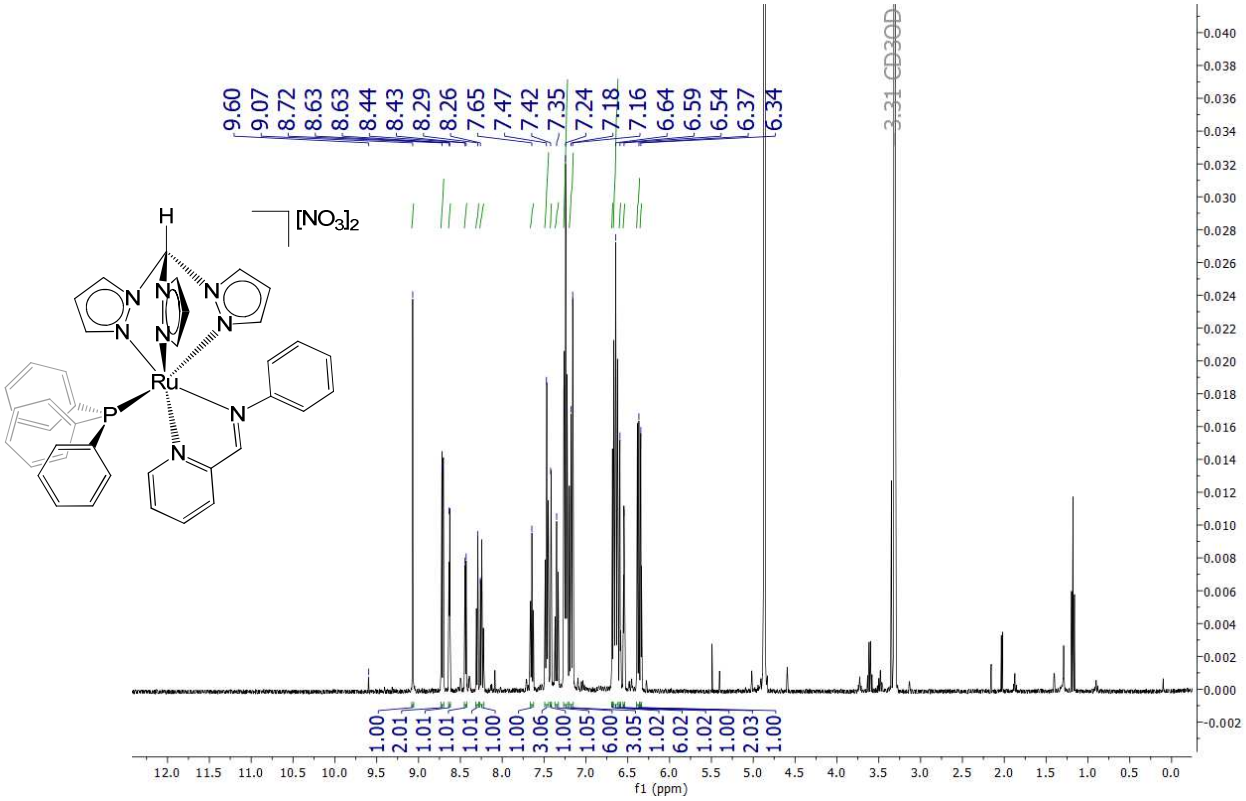

Figure S31. $^{13}C\{^{1}H\}$ NMR spectrum (101 MHz, CD_3OD) of **13**

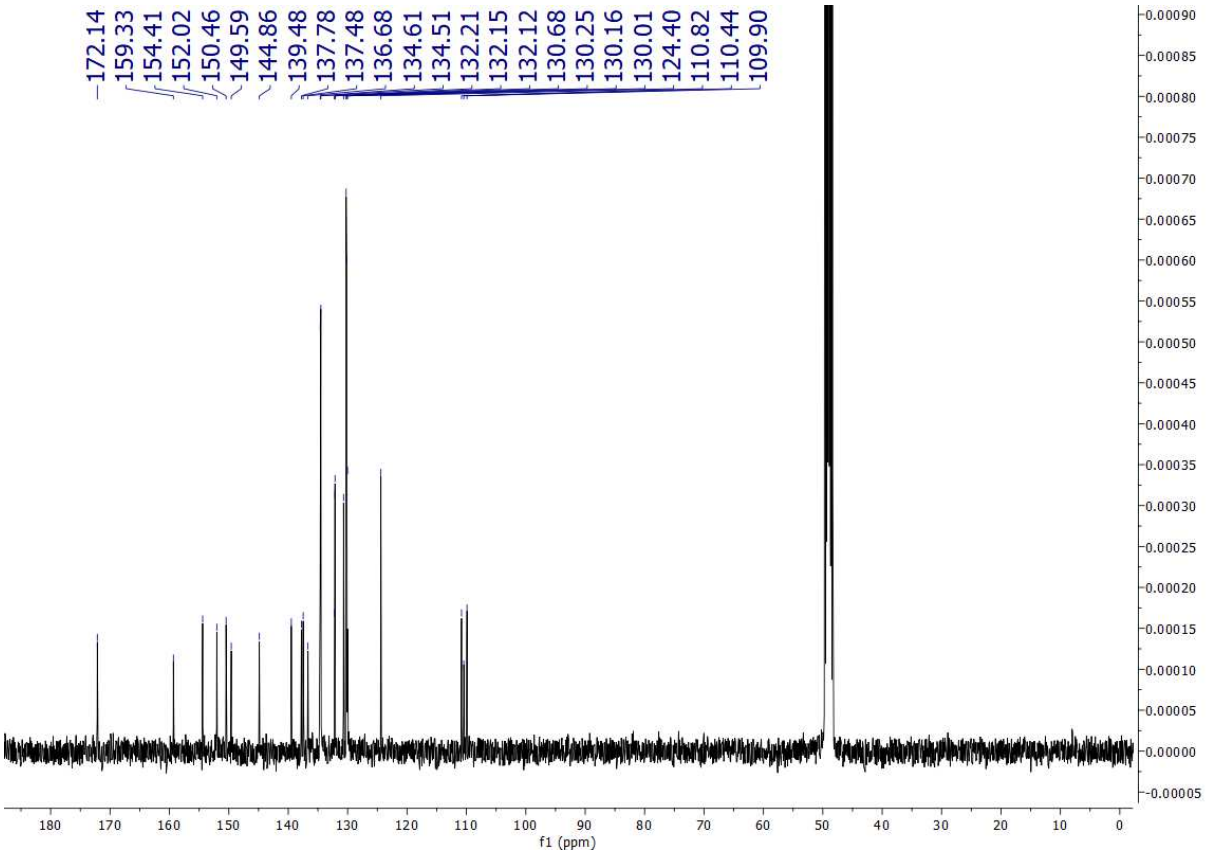

Figure S32. ^{31}P NMR spectrum (162 MHz, CD_3OD) of **13**

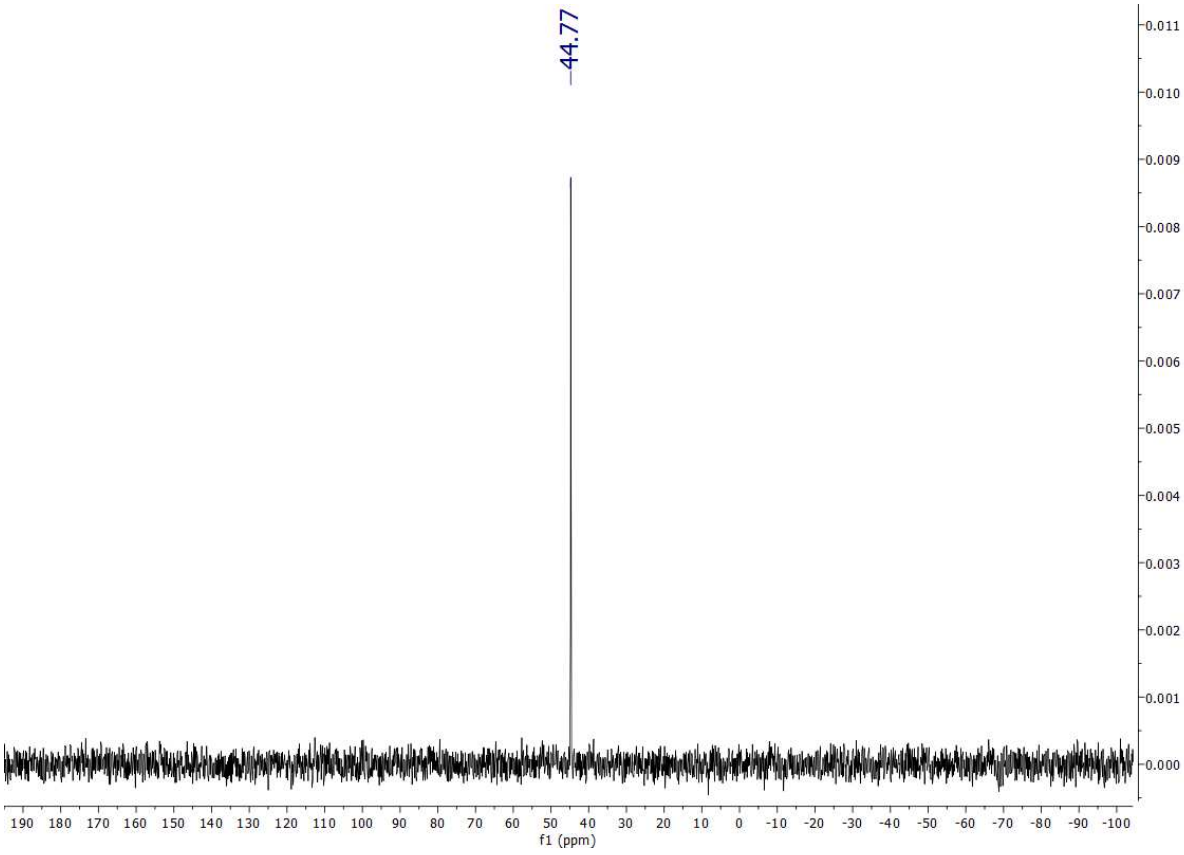

Figure S33. ^{1}H NMR spectrum (401 MHz, CD_3OD) of **14**

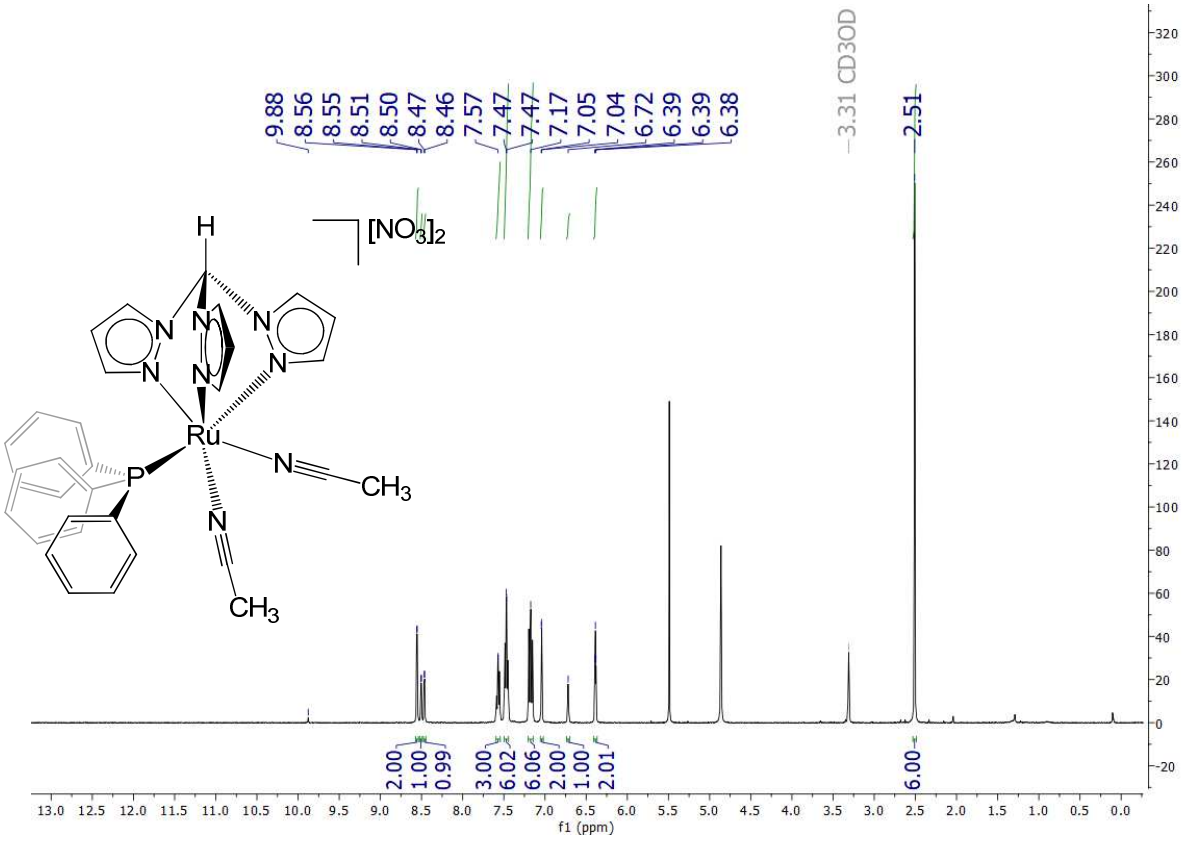

Figure S34. $^{13}C\{^{1}H\}$ NMR spectrum (101 MHz, CD_3OD) of **14**

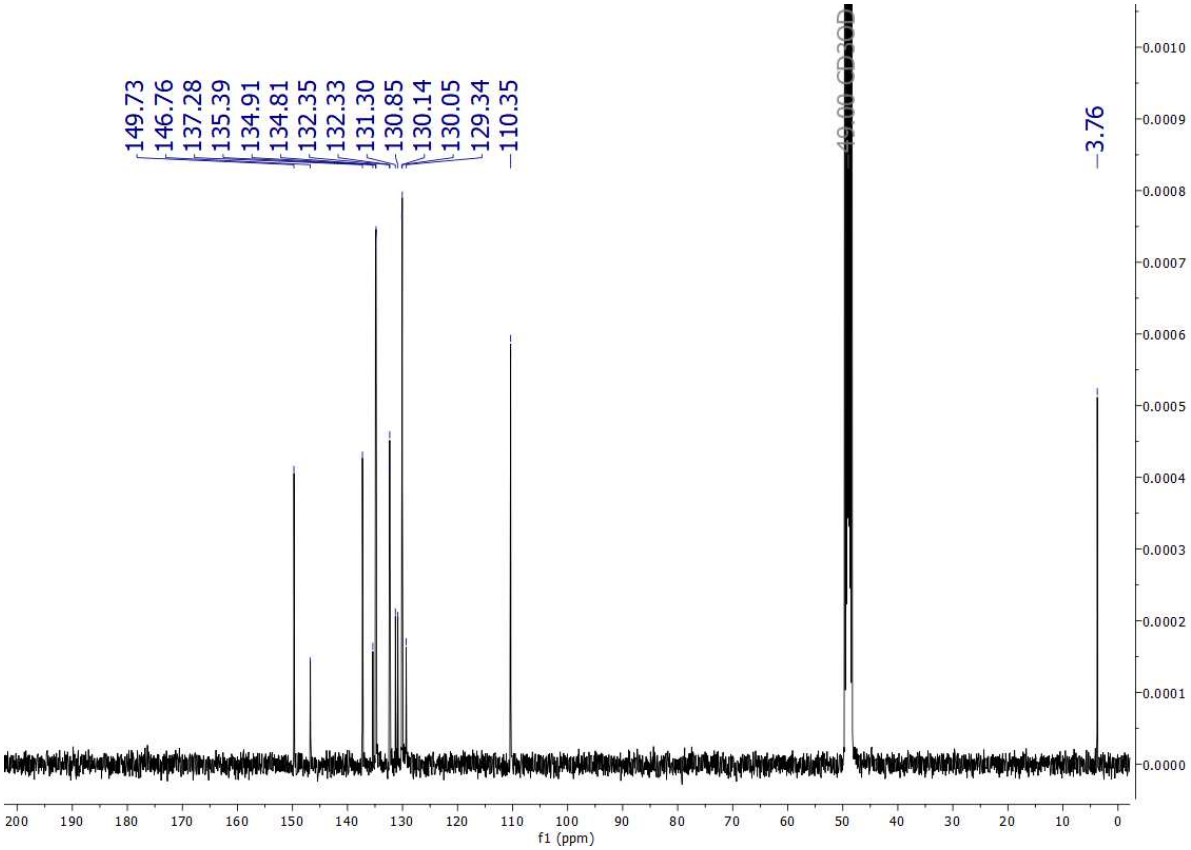

Figure S35. ^{31}P NMR spectrum (162 MHz, CD_3OD) of **14**

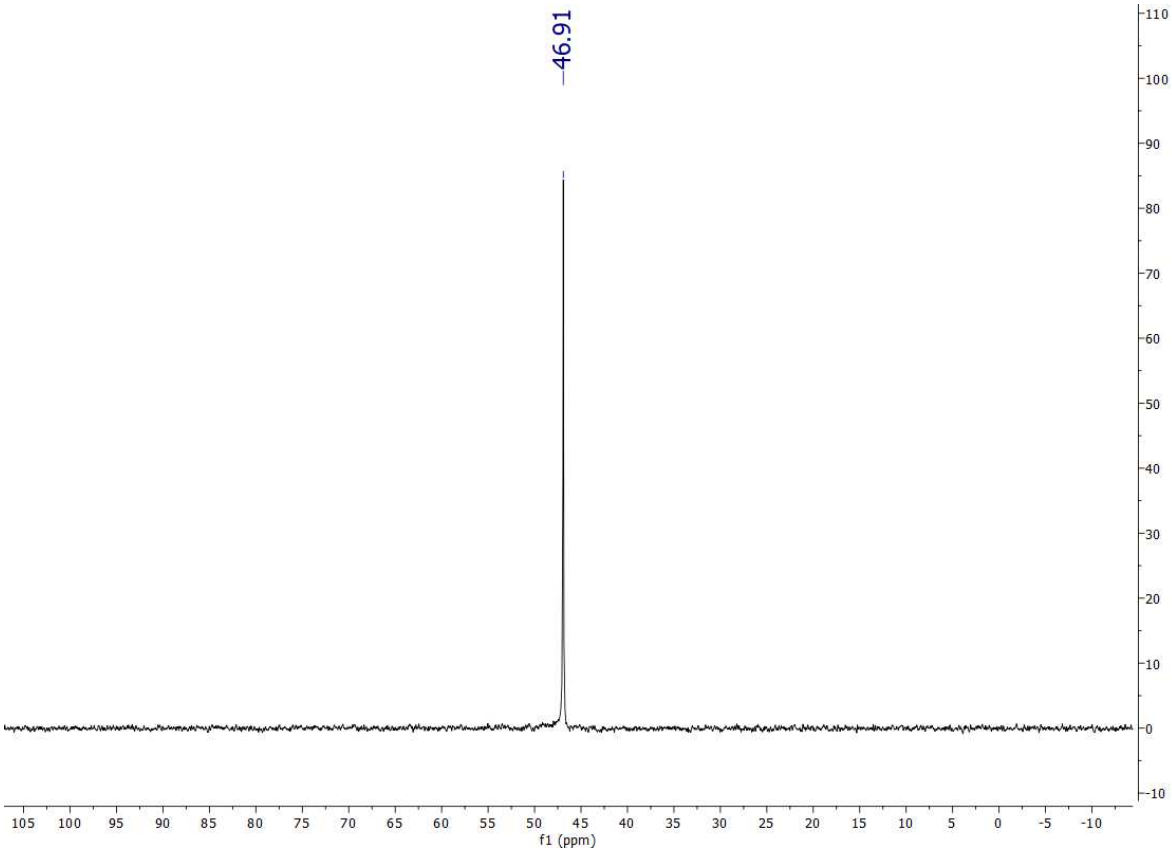

NMR data of complexes in aqueous solutions

Figure S36. Complex [RuCl(κ^3-tpm)(PPh$_3$)(PTA)]Cl, **3**, in DMSO-d$_6$/D$_2$O.

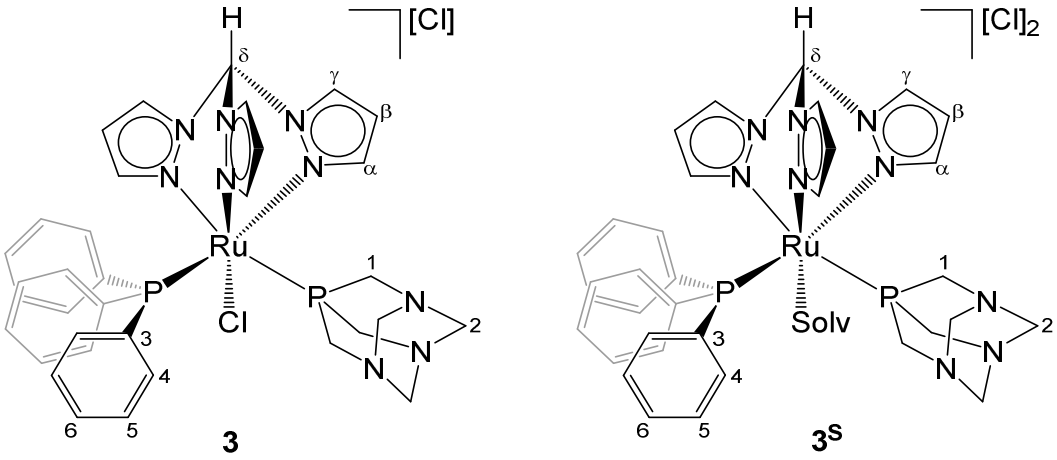

^{1}H NMR (DMSO-d$_6$/D$_2$O, 1:3 v/v ratio): δ/ppm (**3**) = 8.44, 8.39, 8.39 (d, 3H, $^3J_{HH}$ = 2.8 Hz, C$^{\gamma}$H); 8.32, 6.74, 6.34 (d, 3H, $^3J_{HH}$ = 2.3 Hz, C$^{\alpha}$H); 7.66 (m, 6H, C^{4}H); 7.57 (m, 3H, C^{6}H); 7.48 7.57 (m, 3H, C^{5}H); 6.71, 6.33, 6.18 (t, 3H, $^3J_{HH}$ = 2.7 Hz, C$^{\beta}$H); 4.45 (AB spin system, 3H, C^{2}H); 4.31 (AB spin system, 3H, C^{2}H); 3.90 (m, 6H, C^{1}H). δ/ppm (**3^S**) = 8.51, 8.49, 8.49 (m, 3H, C$^{\gamma}$H); 8.33, 7.00, 6.34 (m, 3H, C$^{\alpha}$H); 7.67-7.46 (m, 15H, C^{4}H + C^{5}H + C^{6}H); 6.76, 6.40, 6.34 (m, 3H, C$^{\beta}$H); 4.56-4.25 (m, 6H, C^{2}H); 3.96-3.82 (m, 6H, C^{1}H). *C$^{\delta}$H not observed.* ^{31}P{^{1}H} NMR (D$_2$O): δ/ppm = 43.5 (d, $^2J_{PP}$= 34.9 Hz, PPh$_3$); -31.5 (d, $^2J_{PP}$= 35.0 Hz, PTA) (**3**), **3^S** not observed. **3/3^S** ratio (from ^{1}H NMR) = only A (t$_0$), 10.0 (48h).

Figure S37. Complex [RuCl(κ^3-tpm)(PPh$_3$)(PH$_2$Fc)]Cl, **4**, in DMSO-d$_6$/D$_2$O.

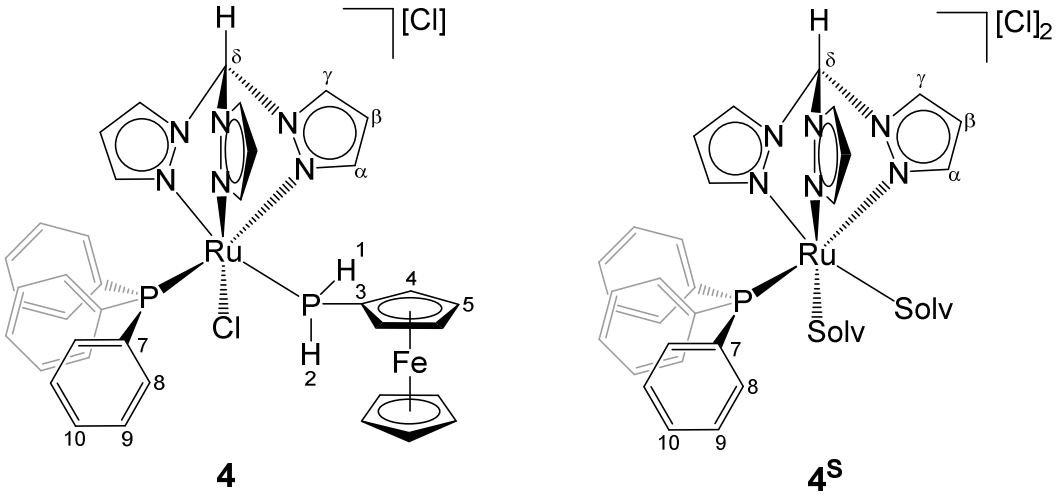

4 **4^S**

^{1}H NMR (DMSO-d$_6$/D$_2$O, 1:2 v/v ratio): δ/ppm (**4**) = 9.52 (s, 1H, C$^{\delta}$H); 8.44, 8.30 (d-br, 3H, C$^{\gamma}$H); 7.70, 7.06, 6.66, (d-br, 3H, C$^{\alpha}$H); 7.52 (m, 3H, C^{10}H); 7.43 (m, 6H, C^{8}H); 7.32 (m, 6H, C^{9}H); 6.47, 6.39, 6.08 (t-br, 3H, C$^{\beta}$H); 5.58 (d, 1H, P-H^1, $^1J_{PH}$ = 370.3 Hz); 5.53 (d, 1H, P-H^2, $^1J_{PH}$ = 355.8 Hz); 4.30, 4.29 (s, 2H, C^{5}H, C$^{5'}$H); 4.17 (s, 5H, Cp); 3.91 (d, 2H, C^{4}H, C$^{4'}$H, $^3J_{PH}$ = 40.1 Hz). ^{31}P{^{1}H} NMR (DMSO-d$_6$/D$_2$O, 1:2 v/v ratio): δ/ppm = 47.1 (d, $^2J_{PP}$ = 36.1, PPh$_3$); -3.9 (d, $^2J_{PP}$ = 35.1, PH$_2$Fc). The ^{1}H NMR spectrum recorded after 48 h appeared rather complex, though it clearly indicated the complete disappearance of **4**. The ^{31}P NMR spectrum revealed the formation of at least two new Ru-PPh$_3$ species lacking the PH$_2$Fc ligand, one of which is likely **4^S**. ^{31}P{^{1}H} NMR (DMSO-d$_6$/D$_2$O, 1:2 v/v ratio): δ/ppm = 60.3 (s), 38.1 (s), −99.2 (s).

The absence of free FcPH$_2$ was assessed by independently characterizing this compound in DMSO-d$_6$/D$_2$O (3:1 v/v ratio), where it showed a ^{31}P NMR signal at −146.8 ppm (m). After this solution was kept at 37 °C for 48 h, the subsequent ^{31}P spectrum displayed only a very weak signal corresponding to FcPH$_2$. This observation suggests that FcPH$_2$ undergoes degradation under the investigated conditions.

Figure S38. ^{1}H NMR spectrum (401 MHz) of **4** in DMSO-d_6/D_2O (1:2 v/v ratio) after 5 minutes (A) and 48 h (B) from dissolution

A

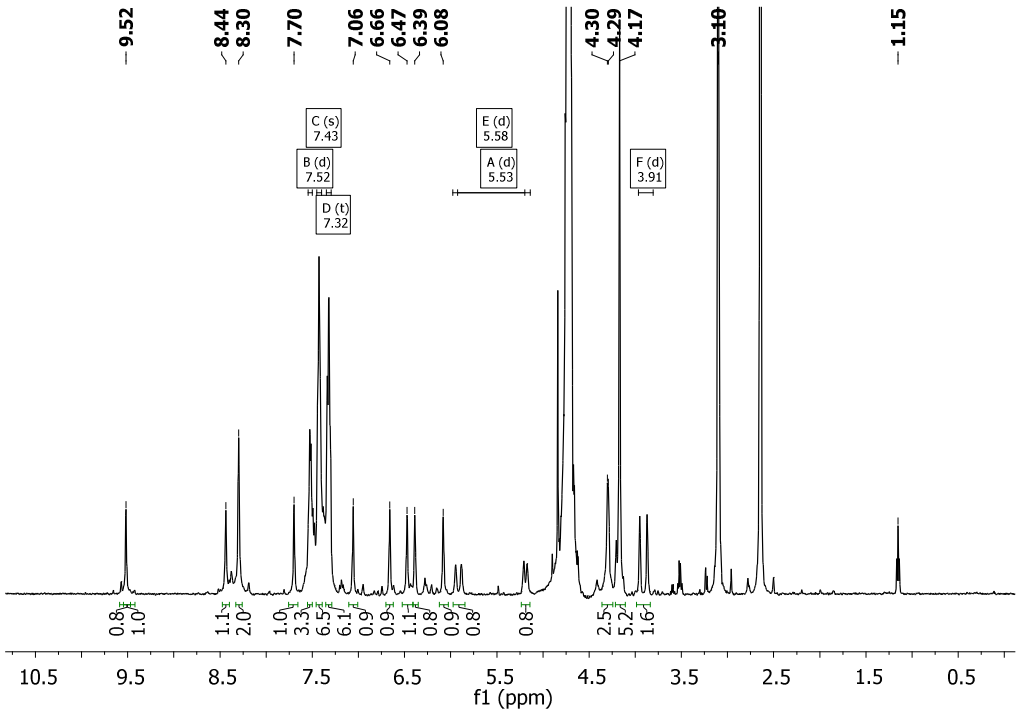

B

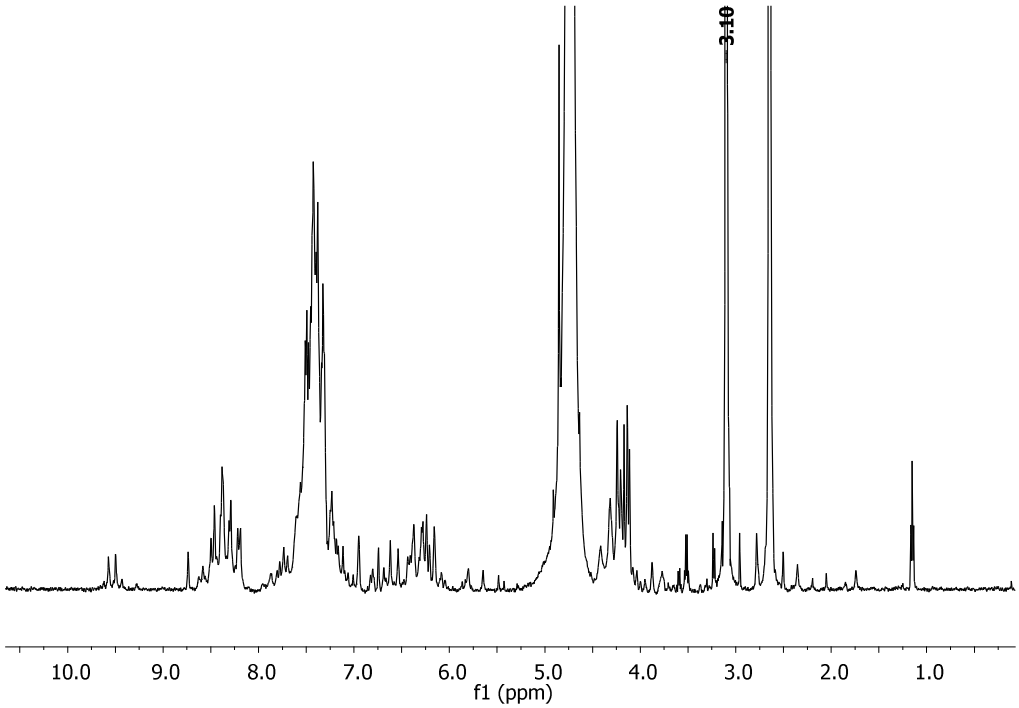

Figure S39. ^{31}P NMR spectrum (162 MHz) of **4** in DMSO-d_6/D_2O (1:2 v/v ratio) after 5 minutes (A) and 48 h (B) from dissolution.

A

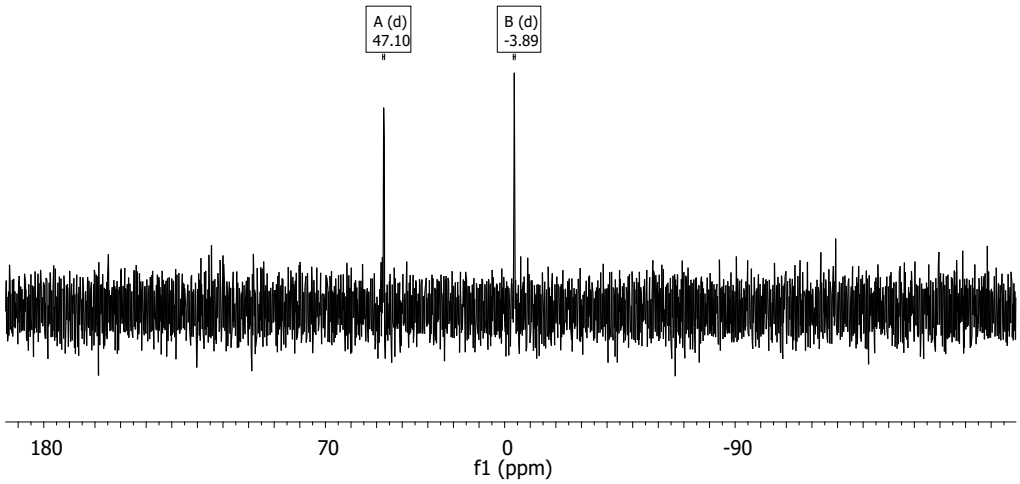

B

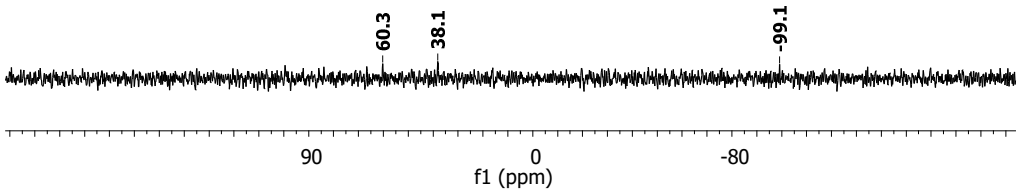

Figure S40. ^{31}P NMR spectrum (162 MHz) of $FcPH_2$ in DMSO-d_6/D_2O (3:1 v/v ratio) after 5 minutes (A) and 48 h (B) from dissolution.

A

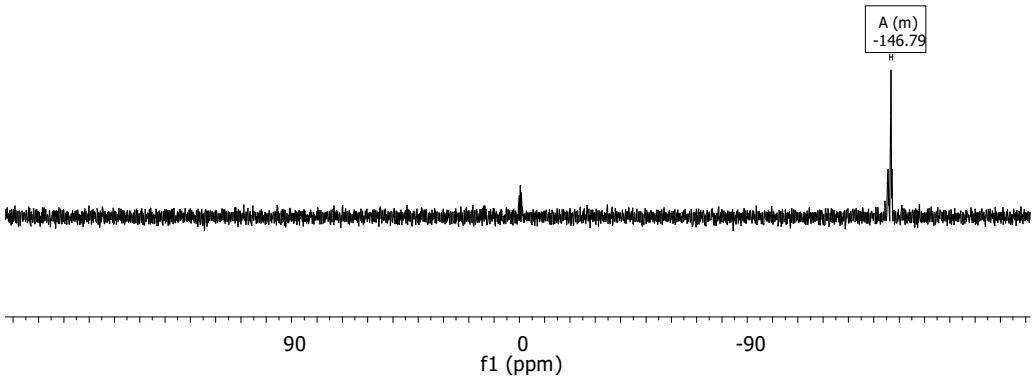

B

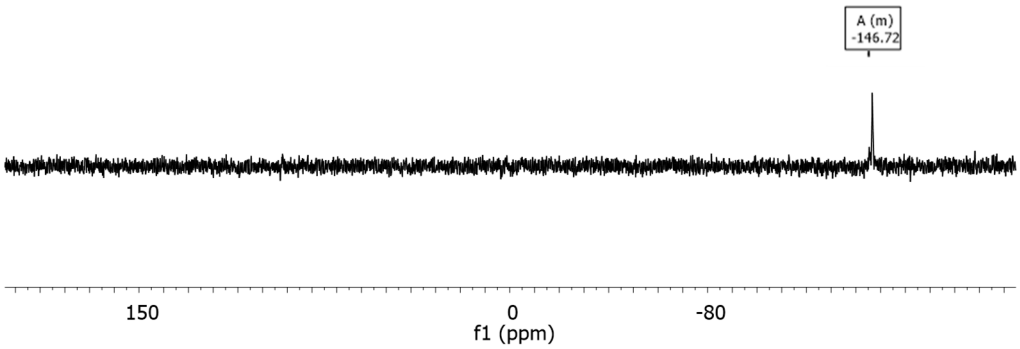

Figure S41. Complex [RuCl(κ^3-tpm){N(NH)CMe(CH)$_2$}(PPh$_3$)]Cl, **5**, in D_2O.

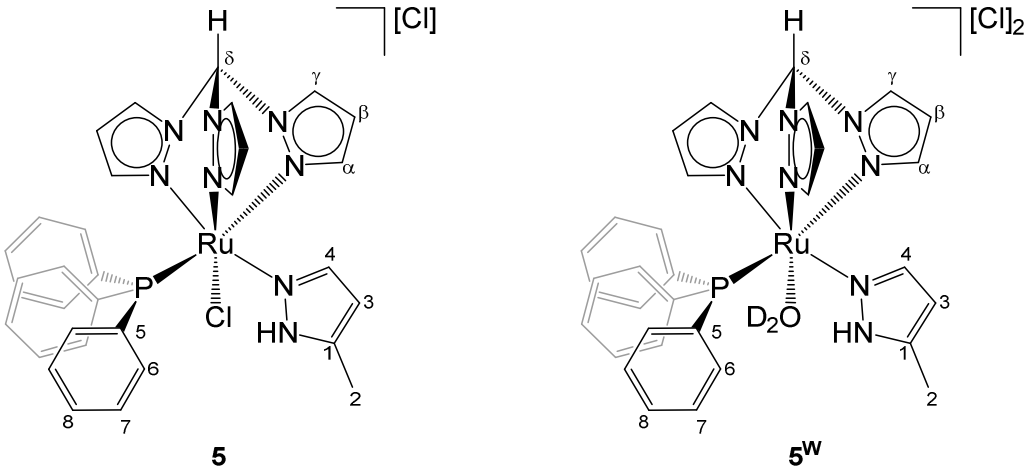

^{1}H NMR (D_2O): δ/ppm (**5**) = 8.39 (d, 3H, $^3J_{HH}$ = 2.9 Hz, C$^{\gamma}$H); 8.34 (m, 2H, C$^{\gamma}$H); 7.46, 7.07(d-br, 2H, C$^{\alpha}$H); 7.44 (m, 3H, C^{8}H); 7.27 (t, 6H, $^3J_{HH}$ = 7.1 Hz, C^{7}H); 6.97 (m, 8H, C$^{\alpha}$H + C^{6}H + C^{4}H); 6.51, 6.30, 6.13 (t-br, 3H, C$^{\beta}$H); 6.11 (s-br, 1H, C^{3}H); 2.15 (s, 3H, C^{2}H). δ/ppm (**5^W**) = 8.44, 8.41, 8.39 (d, 3H, $^3J_{HH}$ = 2.8 Hz, C$^{\gamma}$H); 7.50 (m, 4H, C^{8}H + C^{4}H); 7.32 (t, 6H, $^3J_{HH}$ = 7.1 Hz, C^{7}H); 7.06, 7.01, 6.97 (d-br, 3H, C$^{\alpha}$H); 6.94 (m, 6H, C^{6}H); 6.58, 6.32 (t-br, 2H, C$^{\beta}$H); 6.18 (m, 4H, C$^{\beta}$H + C^{3}H); 2.20 (s, 3H, C^{2}H). ^{31}P{^{1}H} NMR (D_2O): δ/ppm = 49.6 (**5**), 51.2 (**5^W**). **5/5^W** ratio (from ^{13}P NMR) = only **5** (t_0), only **5^W** (48h).

Figure S42. Complex [RuCl(κ^3-tpm)(PPh$_3$)(κ^1*N*-NH$_2$(CH$_2$)$_2$OH)]Cl, **6**, in D$_2$O

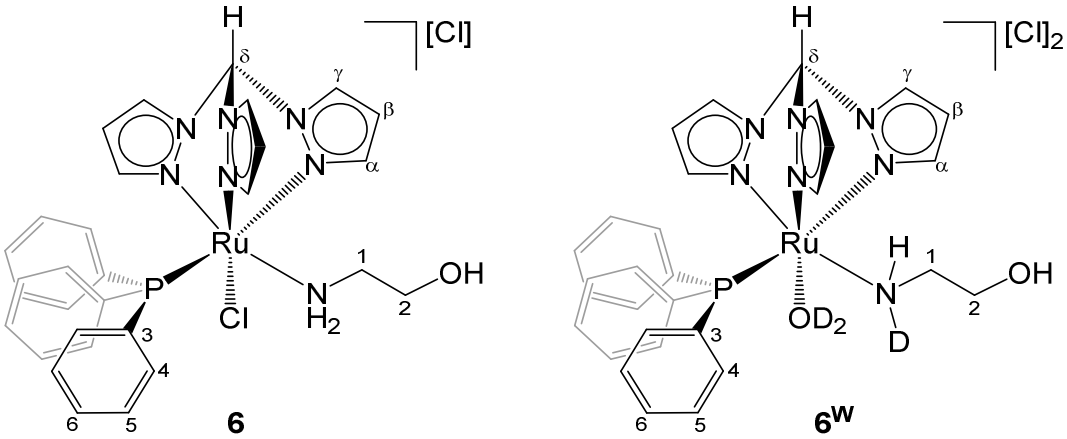

^{1}H NMR (D$_2$O): δ/ppm (**6**) = 9.52 (s, 1H, C$^{\delta}$H); 8.41, 8.38, 8.35 (d, 3H, $^3J_{HH}$ = 2.9 Hz, C$^{\gamma}$H); 8.21, (d, 1H, $^3J_{HH}$ = 2.2 Hz, C$^{\alpha}$H); 7.53-7.02 (m, 17H, C^{6}H + C$^{\alpha}$H + C^{4}H + C^{5}H); 6.67, 6.24, 6.19 (t, 3H, $^3J_{HH}$ = 2.7 Hz, C$^{\beta}$H); 3.78-2.11 (m, 2H, *ethanolamine*). *OH and NH$_2$ not observed.* δ/ppm (**6^W**) = 9.42 (s, 1H, C$^{\delta}$H); 8.37, 8.35, 8.27 (d, 3H, $^3J_{HH}$ = 2.8 Hz, C$^{\gamma}$H); 8.16, 7.17, 6.93 (d, 3H, $^3J_{HH}$ = 2.3 Hz, C$^{\alpha}$H); 7.52 (m, 3H, C^{6}H); 7.93 (m, 6H, C^{4}H); 7.12 (m, 6H, C^{5}H); 6.62, 6.25, 6.13 (t, 1H, $^3J_{HH}$ = 2.6 Hz, C$^{\beta}$H); 3.90 (t-br, 1H, NH$_2$); 3.78 (m, 1H, C^{2}H);); 3.60 (m, 1H, C^{2}H); 2.73 (m, 1H, C^{1}H); 2.11 (m, 1H, C^{1}H). *OH not observed.* ^{31}P{^{1}H} NMR (D$_2$O): δ/ppm = 52.8 (**6^W**), 54.04 (**6**). **6^W/6** ratio (from ^{1}H NMR) = 9.0 (t$_0$), 9.5 (after 48h). In DMSO-d$_6$/DMEM-d (0.14/0.56 mL): **6^W/6** ratio (from ^{31}P NMR) = 2.7 (t$_0$), 5.3 (after 24h).

Figure S43. Complex [RuCl(κ^3-tpm)(PPh$_3$)(NH$_2$(CH$_2$)$_2$C(CH)$_4$COH)]Cl, **7**, in D$_2$O

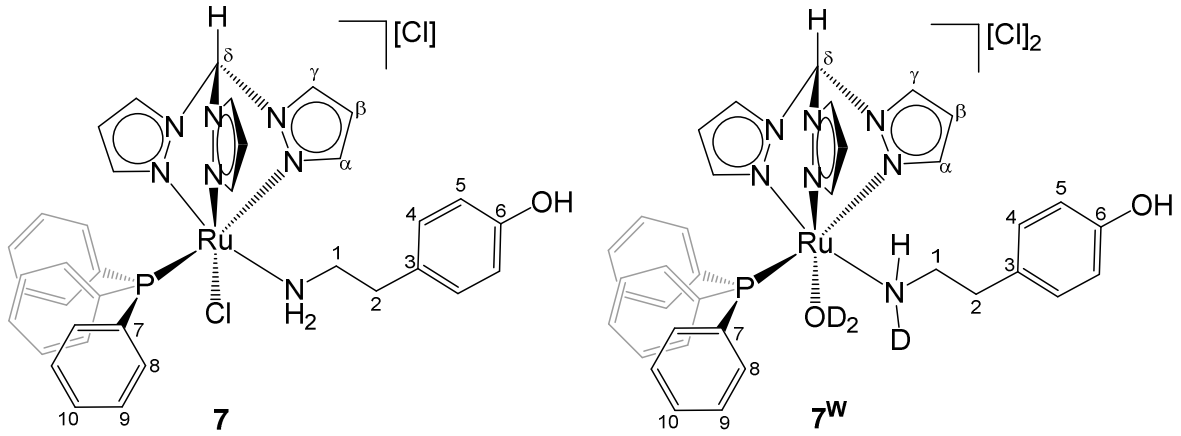

^{1}H NMR (D$_2$O): δ/ppm (**7**) = 9.38 (s, 1H, C$^{\delta}$H); 8.32, 8.29, 8.26 (d, 3H, $^3J_{HH}$ = 2.9 Hz, C$^{\gamma}$H); 7.85, 7.27, 6.83 (d, 3H, $^3J_{HH}$ = 2.2 Hz, C$^{\alpha}$H); 7.46 (m, 3H, C^{10}H); 7.33 (m, 6H, C^{8}H); 7.25 (m, 6H, C^{9}H); 6.87-6.74 (m, 4H, C^{4}H + C^{5}H); 6.57, 6.20, 6.10 (t, 3H, $^3J_{HH}$ = 2.6 Hz, C$^{\beta}$H); 3.10-2.24 (m, 6H, *tyramine*). *OH not observed*. δ/ppm (**7^w**) = 9.49 (s, 1H, C$^{\delta}$H); 8.40, 8.35, 8.34 (d, 3H, $^3J_{HH}$ = 2.9 Hz, C$^{\gamma}$H); 7.97, 6.95, 6.84 (d, 3H, $^3J_{HH}$ = 2.2 Hz, C$^{\alpha}$H); 7.50 (m, 3H, C^{10}H); 7.35 (m, 6H, C^{8}H); 7.09 (m, 6H, C^{9}H); 6.87-6.76 (m, 4H, C^{4}H + C^{5}H); 6.65, 6.22, 6.17 (t, 3H, $^3J_{HH}$ = 2.7 Hz, C$^{\beta}$H); 2.90 (t-br, 1H, NH$_2$); 2.52-2.42 (m, 1H, C^{2}H + C^{1}H); 2.27 (m, 1H, C^{1}H). *OH not observed*. ^{31}P{^{1}H} NMR (D$_2$O): δ/ppm = 54.1 (**7^W**), 52.8 (**3**). **7^W/7** ratio (from ^{1}H NMR) = 25.0 (t$_0$), 25.0 (after 48h). In DMSO-d$_6$/DMEM-d (0.14/0.56 mL): **7^W/7** ratio (from ^{31}P NMR) = 0.6 (t$_0$), 2.0 (after 24h).

Figure S44. ^{1}H NMR spectrum (401 MHz) of **7** in D_2O (Cl^-/D_2O exchange) after 5 minutes (A) and 10 minutes (B) from dissolution.

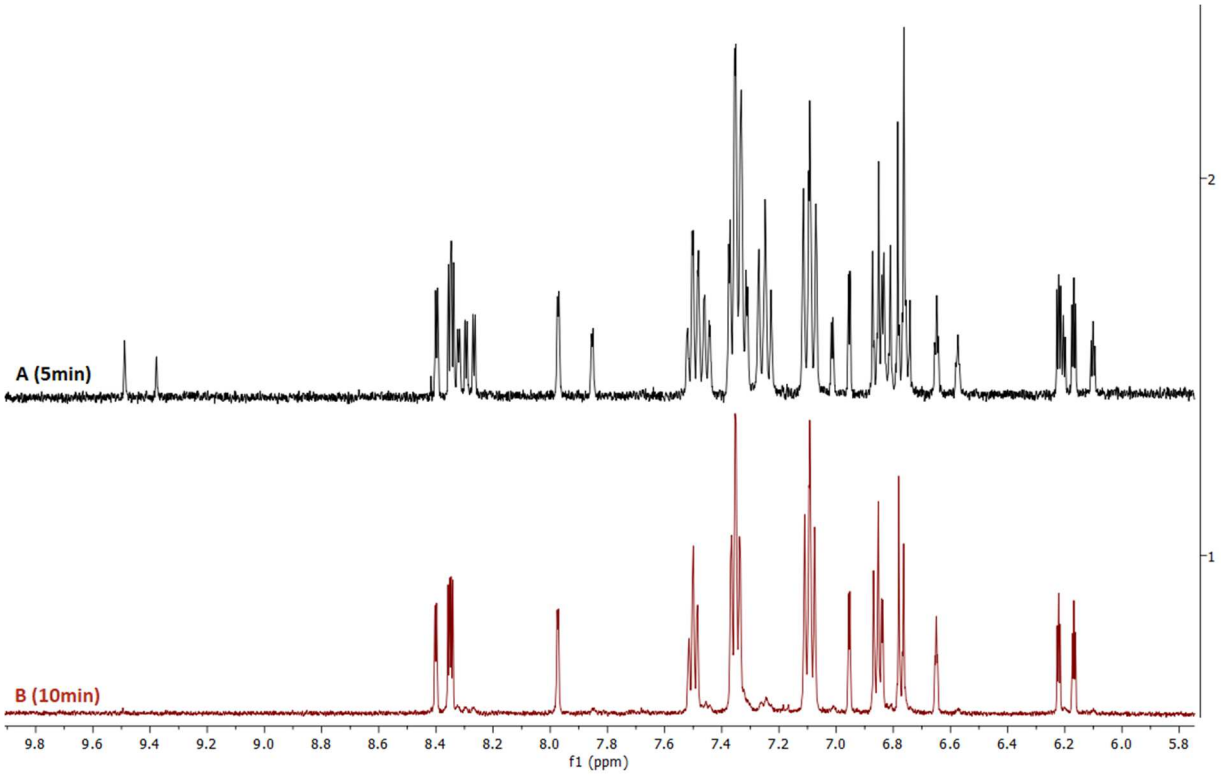

Figure S45. ^{1}H NMR spectrum (401 MHz) of **7** in CD_3OD: A, untreated compound; B, solid isolated after dissolution in H_2O.

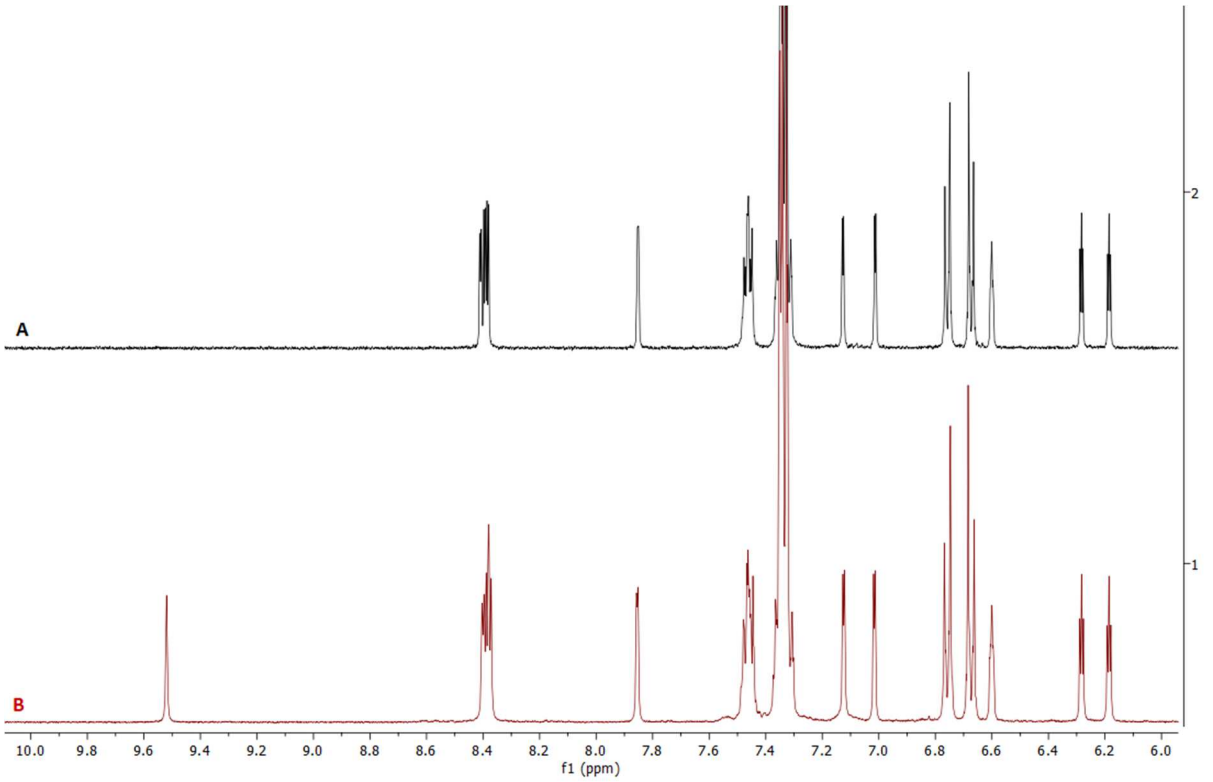

Figure S46. Complex [RuCl(κ^3-tpm)(PPh$_3$)(NH(CH$_2$)$_4$NH)]Cl, **8**, in D$_2$O

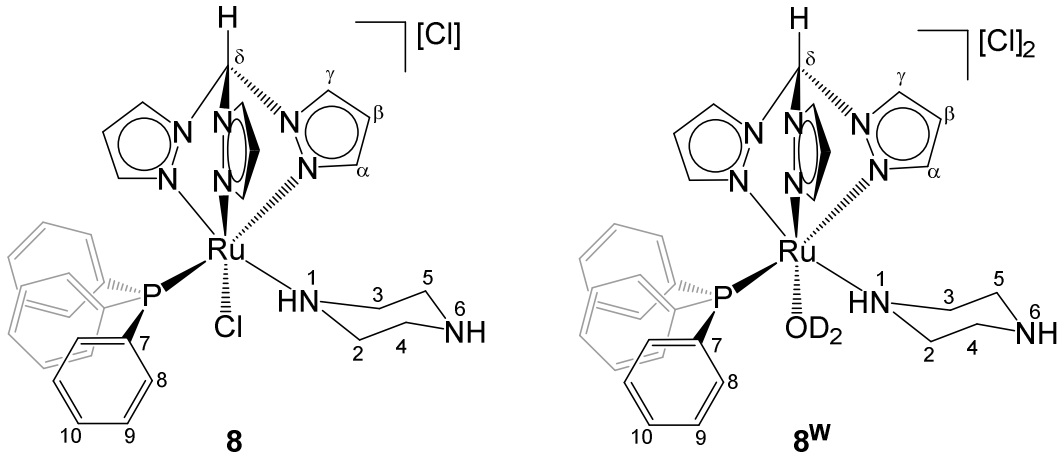

^{1}H NMR (D$_2$O): δ/ppm (**8**) = 8.46-8.49 (m, 3H, C$^{\gamma}$H); 8.35, 6.90 (d-br, 2H, C$^{\alpha}$H); 7.60-7.20 (m, 16H, C$^{\alpha}$H + C^{10}H + C^{8}H + C^{9}H); 6.69, 6.26, 6.22 (t-br, 3H, C$^{\beta}$H); 6.28-1.96 (m, 8H, *Cy*-H). *C$^{\delta}$H and NH not observed.* δ/ppm (**8^w**) = 8.46, 8.44, 8.41 (d, 3H, $^3J_{HH}$ = 2.9 Hz, C$^{\gamma}$H); 8.38, 7.32, 6.86 (d-br, 2H, $^3J_{HH}$ = 2.4 Hz, C$^{\alpha}$H); 7.58 (t-br, 3H, C^{10}H); 7.46 (t, 6H, $^3J_{HH}$ = 7.1 Hz, C^{8}H); 7.2. (t-br, 6H, C^{9}H); 6.75, 6.27, 6.26 (t, 3H, $^3J_{HH}$ = 2.6 Hz, C$^{\beta}$H); 2.88 (m, 1H, *Cy*-H); 2.71-2.57 (m, 3H, *Cy*-H); 2.43 (m, 2H, *Cy*-H); 1.97 (m, 2H, *Cy*-H). *C$^{\delta}$H and NH not observed.* ^{31}P{^{1}H} NMR (D$_2$O): δ/ppm = 52.7 (**8^W**), 50.5 (**8**). **8^W/8** ratio (from ^{1}H NMR) = 10.0 (t$_0$), ∞ (after 48h). In DMSO-d$_6$/DMEM-d (0.14/0.56 mL): **8^W/8** ratio (from ^{31}P NMR) = ∞ (t$_0$), ∞ (after 24h). An additional signal was detected in the ^{31}P NMR spectrum (δ/ppm = 38.1 ppm).

Figure S47. Complex Ru(κ^3*N*-tpm)(κ^2*N*-1,10-phenanthroline)(PPh_3)][NO_3]$_2$, **11,** in D_2O

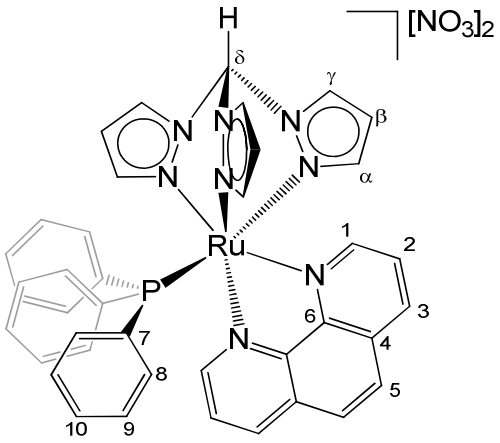

^{1}H NMR (D_2O): δ ppm = 8.75 (d, 2H, $^3J_{HH}$ = 5.3 Hz, C^{1}H); 8.61 (dd, 2H, $^3J_{HH}$ = 8.3 Hz, $^4J_{HH}$ = 1.2 Hz, C^{3}H); 8.56 (d, 2H, $^3J_{HH}$ = 3.0 Hz, C$^\gamma$H); 8.29 (d, 1H, $^3J_{HH}$ = 2.8 Hz, C$^\gamma$H); 8.09 (s, 2H, C^{5}H); 7.77 (dd, 2H, $^3J_{HH}$ = 8.2 Hz, $^3J_{HH}$ = 5.2 Hz, C^{2}H); 7.45 (d, 2H, $^3J_{HH}$ = 2.3 Hz, C$^\alpha$H); 7.33 (t, 3H, $^3J_{HH}$ = 7.1 Hz, C^{10}H); 7.06 (t, 6H, $^3J_{HH}$ = 7.7 Hz, C^{8}H); 6.51 (t, 2H, $^3J_{HH}$ = 2.6 Hz, C$^\beta$H); 6.30 (t, 6H, $^3J_{HH}$ = 2.3 Hz, C^{9}H); 6.29 (m, 8H, C^{8}H + C$^\alpha$H + C$^\beta$H); 6.16 (m, 1H, C$^\alpha$H); 6.14 (m, 1H, C$^\beta$H). *C$^\delta$H not observed.* ^{31}P{^{1}H} NMR (D_2O): δ ppm = 47.6

Figure S48. Complex Ru(κ^3*N*-tpm)(κ^2*N*-$C_5H_4NCH_2NH_2$)(PPh_3)][NO_3]$_2$, **12**, in D_2O

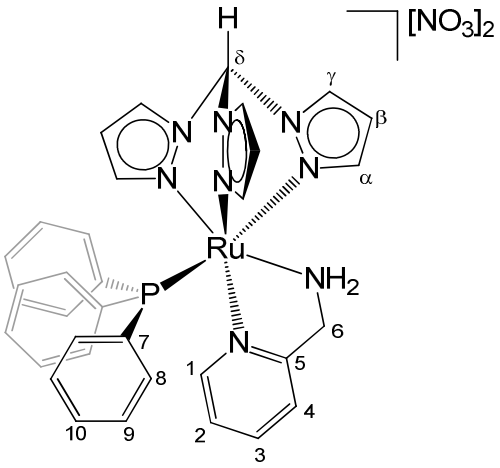

^{1}H NMR (D_2O): δ ppm = 8.41, 8.40, 8.33 (d, 3H, $^3J_{HH}$ = 2.9 Hz, C$^{\gamma}$H); 8.06 (d-br, 1H, $^3J_{HH}$ = 5.7 Hz, C^{1}H); 7.87 (td, 1H, $^3J_{HH}$ = 7.7 Hz, $^4J_{HH}$ = 1.4 Hz, C^{3}H); 7.49 (t, 3H, $^3J_{HH}$ = 7.4 Hz, C^{10}H); 7.43 (d, 1H, $^3J_{HH}$ = 7.9 Hz, C^{4}H); 7.34, 6.95, 6.95 (d, 3H, $^3J_{HH}$ = 2.3 Hz, C$^{\alpha}$H); 7.30 (t, 6H, $^3J_{HH}$ = 7.6 Hz, C^{8}H); 7.24 (t, 1H, $^3J_{HH}$ = 6.6 Hz, C^{2}H); 6.81 (t-br, 6H, C^{9}H); 6.41, 6.32, 6.31 (t, 3H, $^3J_{HH}$ = 2.6 Hz, C$^{\beta}$H); 4.27 (d, 1H, $^2J_{HH}$ = 16.7 Hz, C^{6}H); 3.33 (dd, 1H, $^2J_{HH}$ = 16.7 Hz, $^3J_{HH}$ = 6.0 Hz, C^{6}H). *NH_2 not observed.* ^{31}P{^{1}H} NMR (D_2O): δ ppm = 52.7.

Figure S49. Complex **[**Ru(κ^3*N*-tpm)(κ^2*N*-$C_5H_4NCH{=}NPh$)(PPh_3)][NO_3]$_2$, **13**, in D_2O

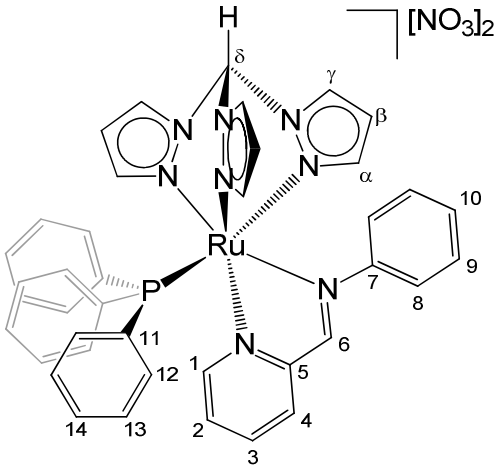

^{1}H NMR (D_2O): δ ppm = 8.96 (s, 1H, C^6H); 8.55, 8.52, 8.43 (d, 3H, $^3J_{HH}$ = 2.9 Hz, $C^{\gamma}H$); 8.34 (d, 1H, $^3J_{HH}$ = 5.6 Hz, C^1H); 8.25 (d, 1H, $^3J_{HH}$ = 7.6 Hz, C^4H); 8.19 (t, 1H, $^3J_{HH}$ = 7.8 Hz, C^3H); 7.53 (ddd, 1H, $^3J_{HH}$ = 7.4 Hz, $^3J_{HH}$ = 5.5 Hz, $^4J_{HH}$ = 1.7 Hz, C^2H); 7.44 (t, 3H, $^3J_{HH}$ = 7.4 Hz, $C^{14}H$); 7.31 (m, 2H, $C^{10}H$ + $C^{\alpha}H$); 7.20 (t-br, 6H, $^3J_{HH}$ = 8.7 Hz, $C^{12}H$ or $C^{13}H$); 7.13 (t, 2H, $^3J_{HH}$ = 7.1 Hz, C^9H); 6.97, 6.76 (d, 2H, $^3J_{HH}$ = 2.3 Hz, $C^{\alpha}H$); 6.65 (t, 6H, $^3J_{HH}$ = 7.8 Hz, $C^{12}H$ or $C^{13}H$); 6.46, 6.41, 6.21 (t, 3H, $^3J_{HH}$ = 2.7 Hz, $C^{\beta}H$); 6.25 (d, 2H, $^3J_{HH}$ = 8.1 Hz, C^8H). $C^{\delta}H$ *not observed*. $^{31}P\{^1H\}$ NMR (D_2O): δ ppm = 44.9

Figure S50. Complex Ru(κ^3*N*-tpm)(NCMe)$_2$(PPh$_3$)][NO$_3$]$_2$, **14** in D$_2$O

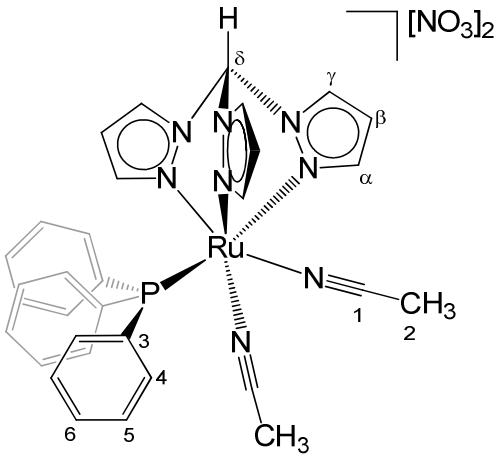

^{1}H NMR (D$_2$O): δ/ppm = 8.37 (d, 2H, $^3J_{HH}$ = 2.9 Hz, C$^{\gamma}$H); 8.33 (d, 1H, $^3J_{HH}$ = 2.7 Hz, C$^{\gamma}$H); 8.27 (d, 1H, $^3J_{HH}$ = 1.8 Hz, C$^{\alpha}$H); 7.55 (m, 3H, C^{6}H); 7.43 (m, 6H, C^{4}H or C^{5}H); 7.21 (m, 6H, C^{4}H or C^{5}H); 7.02 (d, 2H, $^3J_{HH}$ = 2.1 Hz, C$^{\alpha}$H); 6.62 (t-br, 1H, C$^{\beta}$H); 6.27 (t, 2H, $^3J_{HH}$ = 2.6 Hz, C$^{\beta}$H); 2.35 (s, 6H, C^{2}H). C$^{\delta}$H *not observed.* ^{31}P{^{1}H} NMR (D$_2$O): δ ppm = 47.9.

NMR spectra in DMEM-d cell culture medium

Figure S51. ^{1}H NMR spectrum (401 MHz, 5.5-10.5 ppm range) of **10** in DMEM-d cell culture medium after 5 minutes (red) and after 72 hours (green) from dissolution.

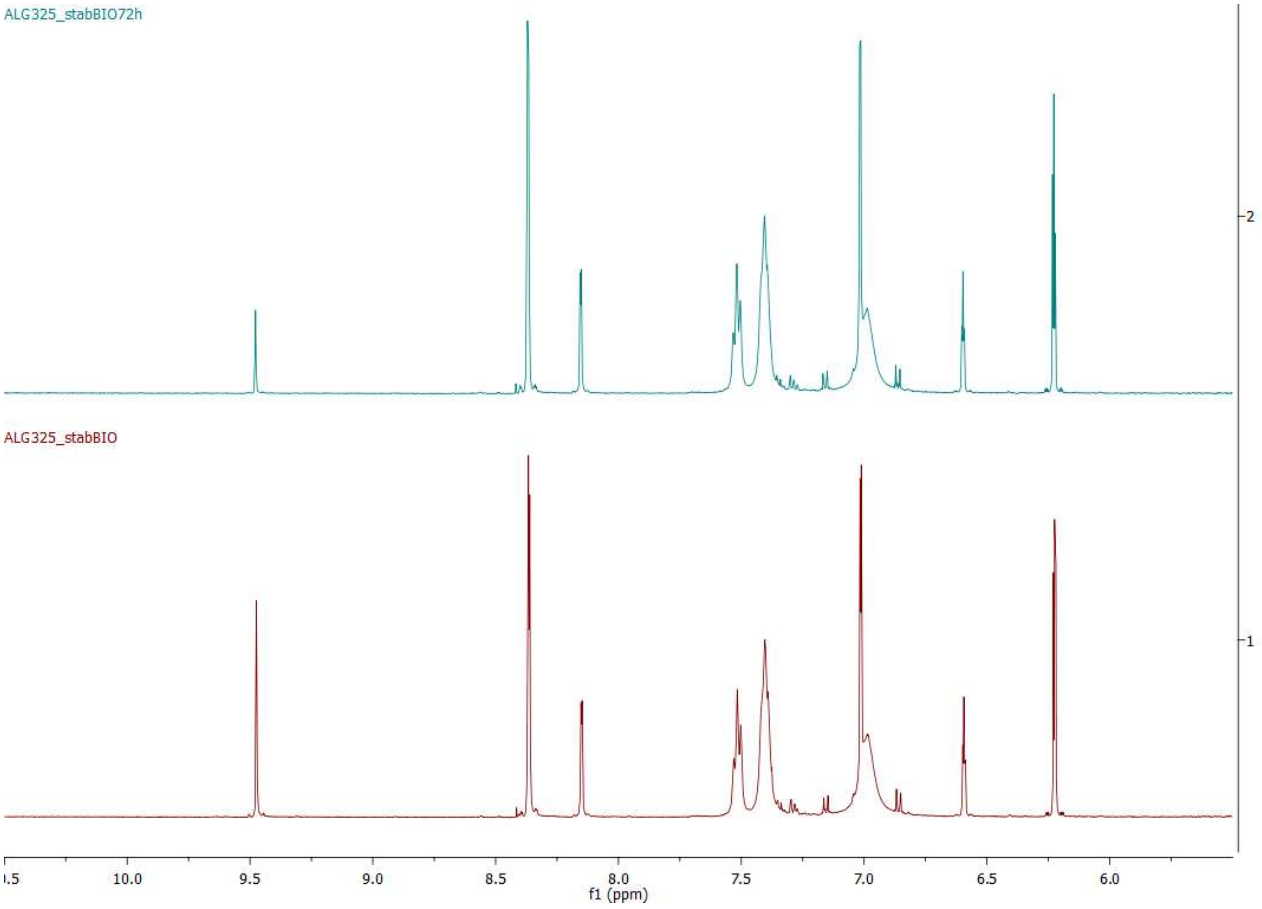

Figure S52. ^{1}H NMR spectrum (401 MHz, 5.5-10.5 ppm range) of **11** in DMEM-d cell culture medium after 5 minutes (red) and after 72 hours (green) from dissolution.

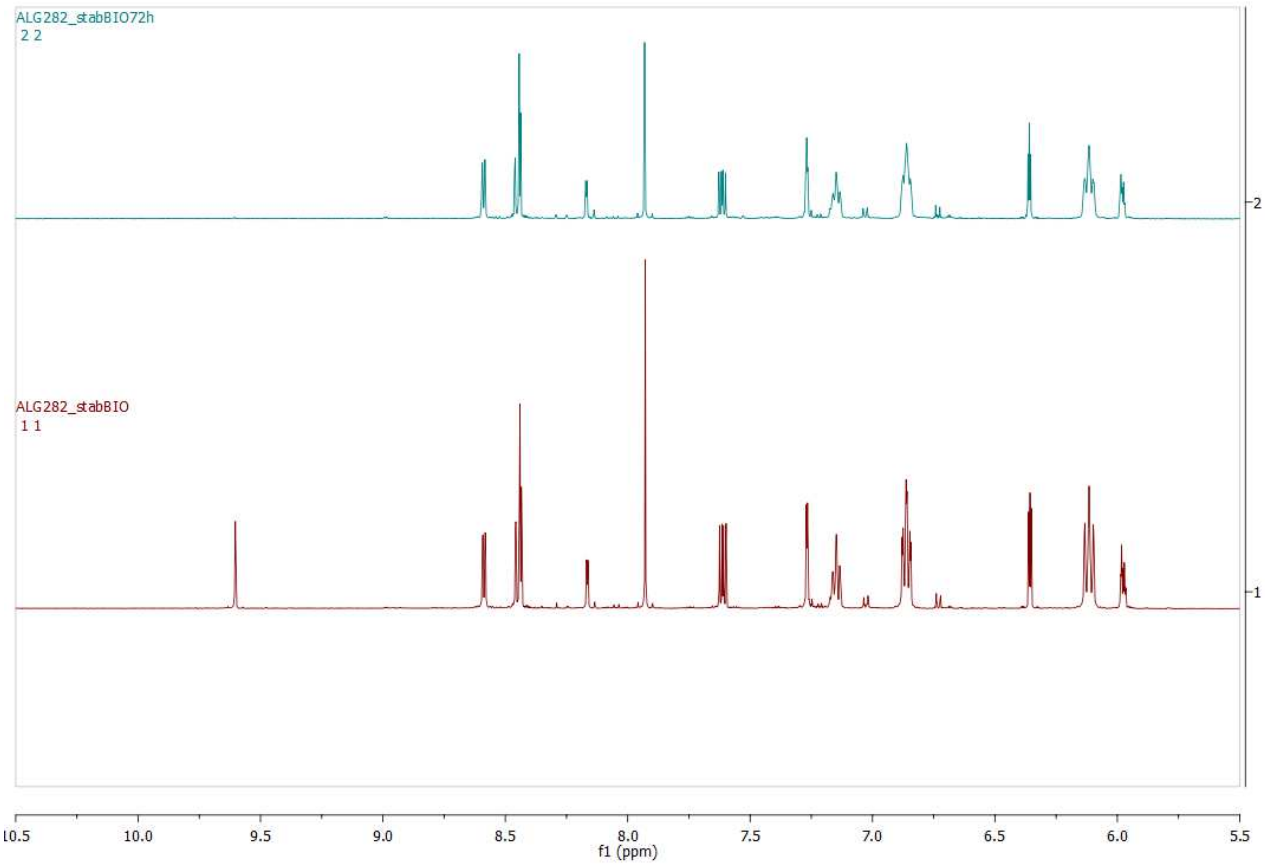

Figure S53. ^{1}H NMR spectrum (401 MHz, .5-10.5 ppm range) of **12** in DMEM-d cell culture medium after 5 minutes (red) and after 72 hours (green) from dissolution.

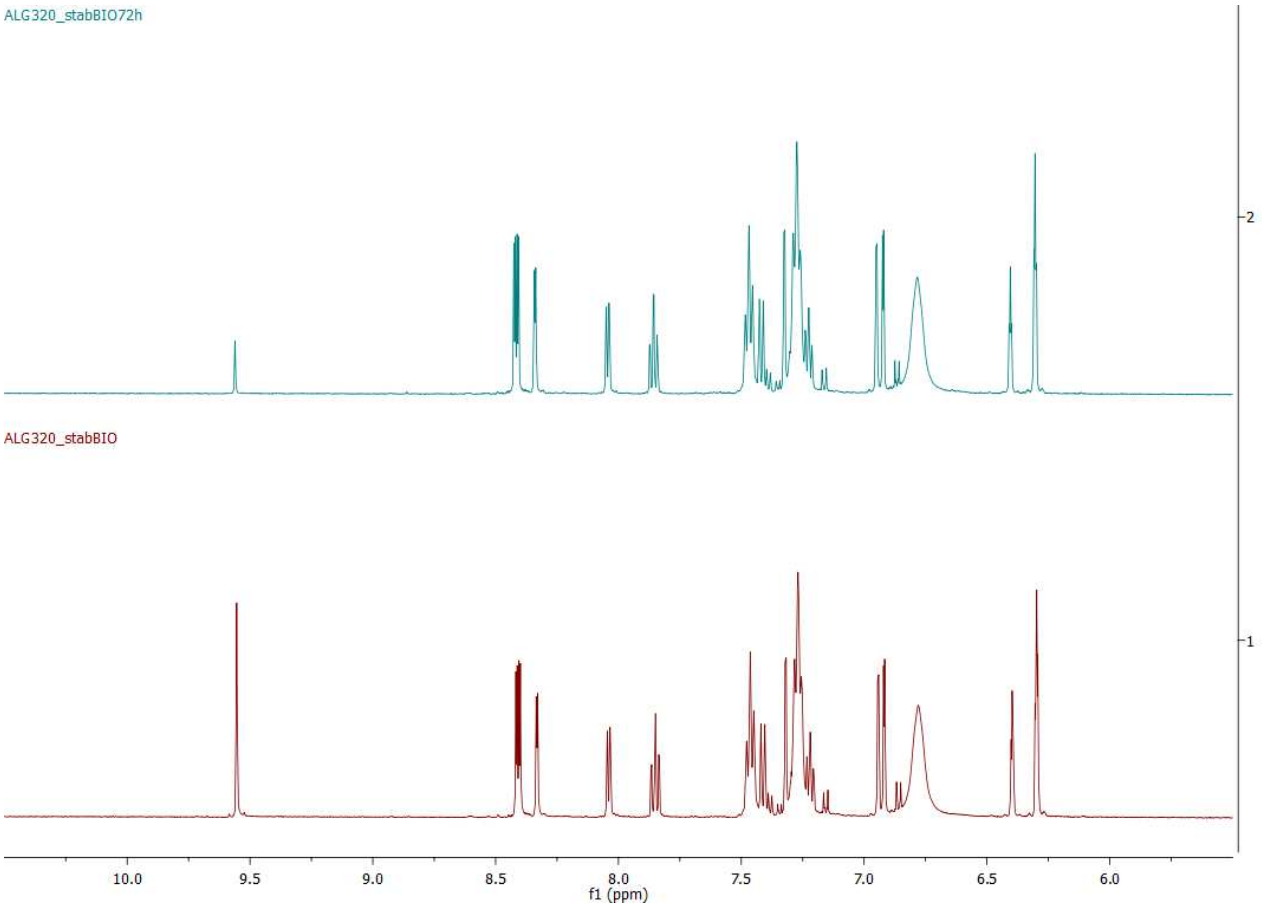

Figure S54. ^{1}H NMR spectrum (401 MHz, the 5.5-10.5 ppm range) of **13** in DMEM-d cell culture medium after 5 minutes (red) and after 72 hours (green) from dissolution.

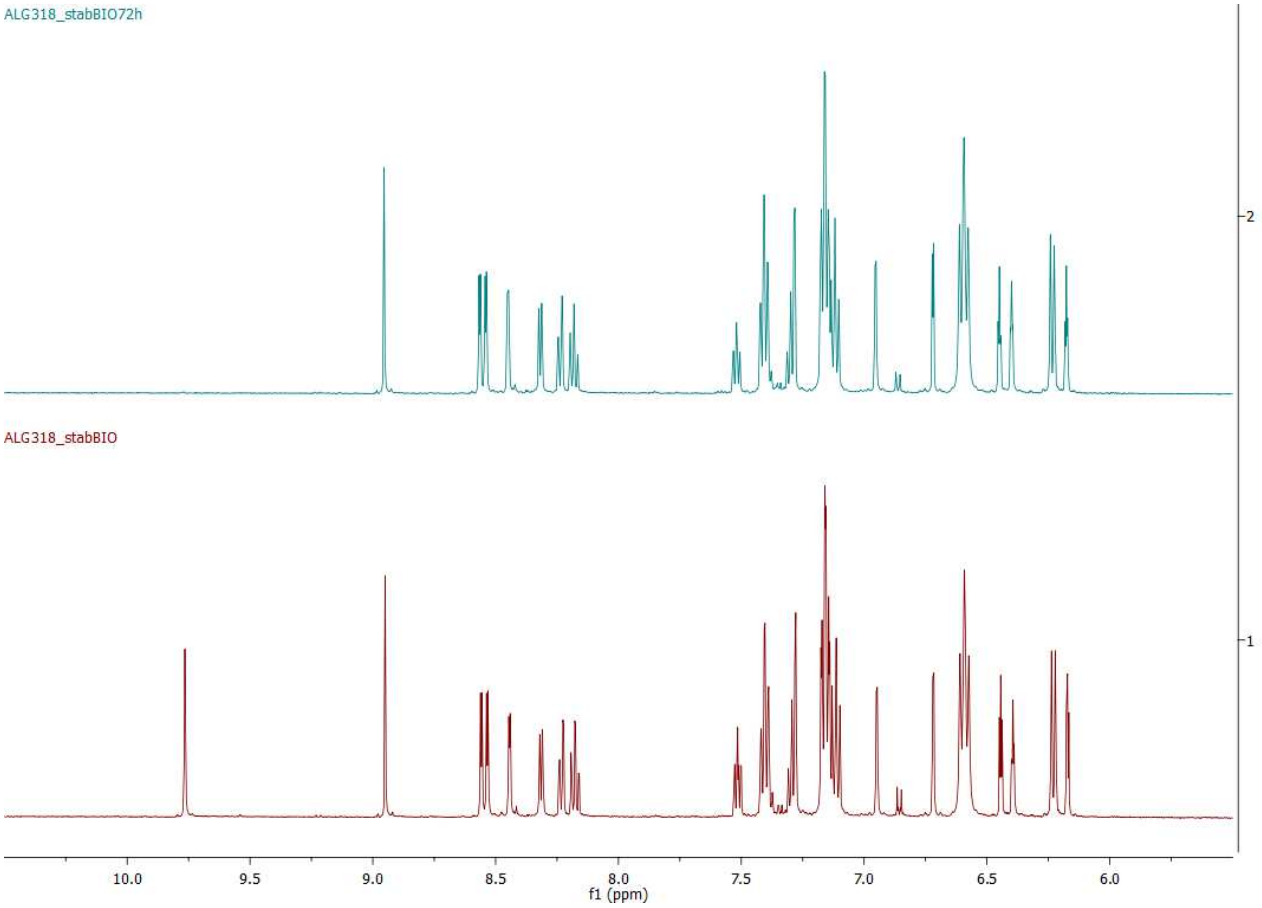

Figure S55. ^{1}H NMR spectrum (401 MHz, 5.5-10.5 ppm range) of **14** in DMEM-d cell culture medium after 5 minutes (red) and after 72 hours (green) from dissolution.

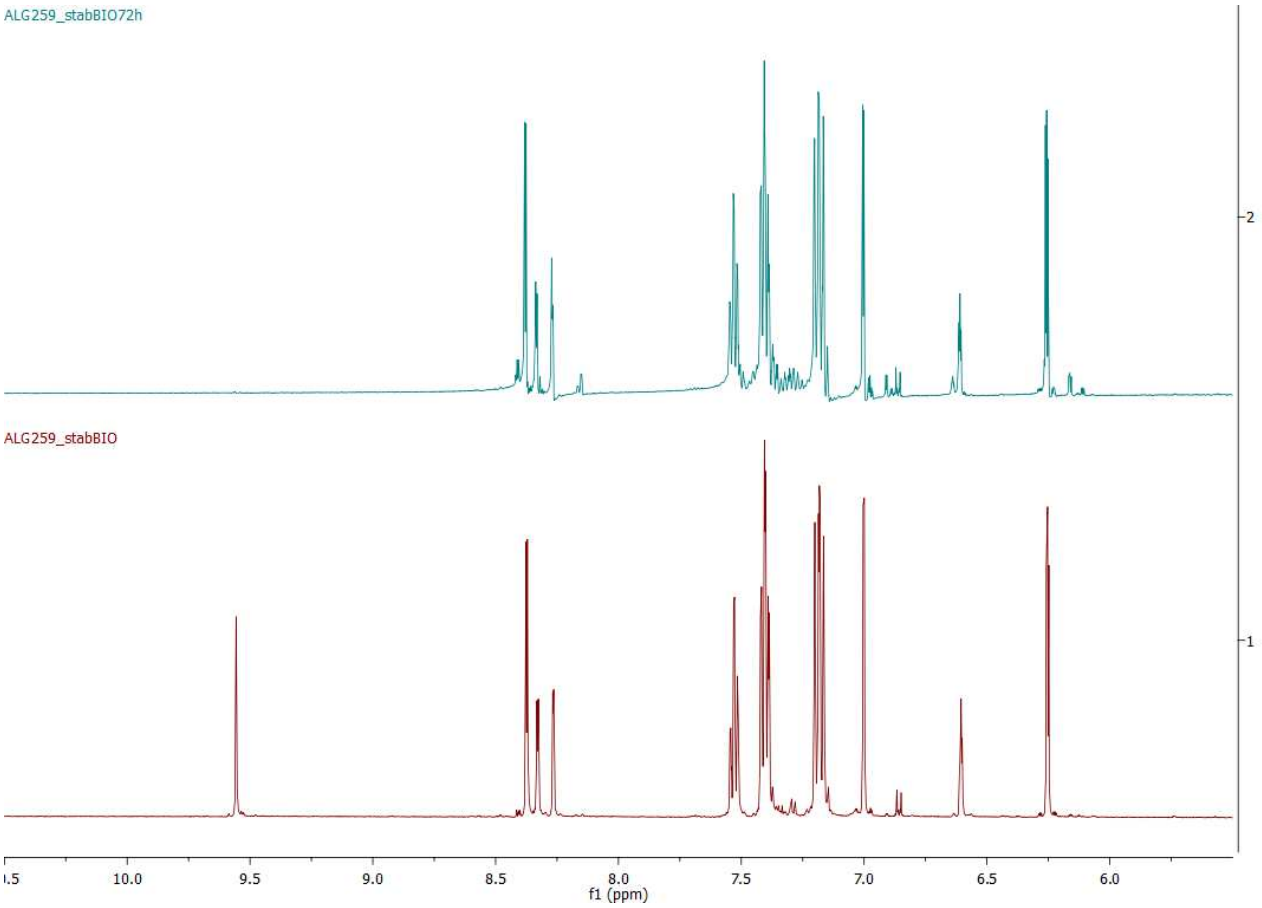

Figure S56. Activation of autophagy in A2780 cells after 24 h incubation with half-cytotoxic concentrations of complexes **1**, **2**, **4**, **13**, **14**, and the reference drug cisplatin. The control cells were only vehicle-treated, while the positive control consisted of the combination of a modulator of autophagic flux, chloroquine and a known mTOR kinase inhibitor (rapamycin).

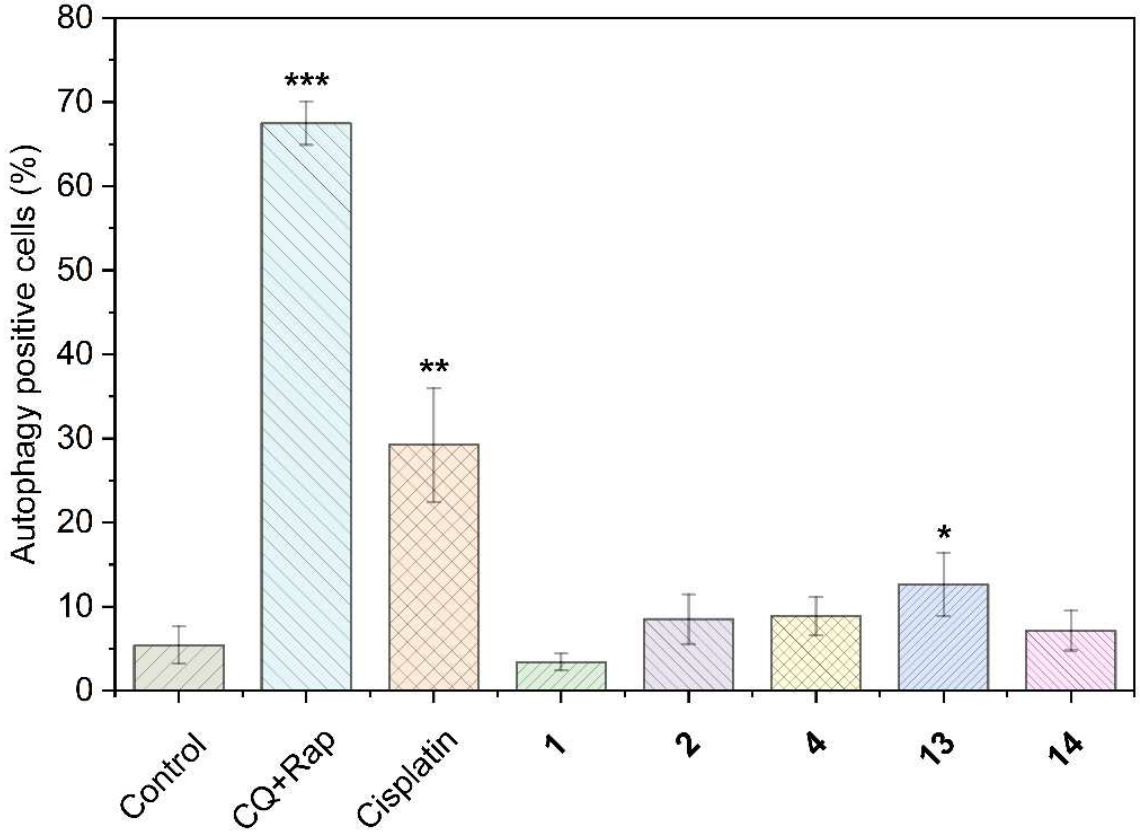

Figure S57. Time dependent UV-vis spectra (recorded every 15 minutes, 2 h 15 min total) of **1** (A, 2.08×10^{-5} M), **2** (B, 9.16×10^{-6} M), **3** (C, 1.59×10^{-5} M), and **13** (D, 3.65×10^{-5} M); 0.01 M NaCac, pH = 7.0, T = 25.0 °C.

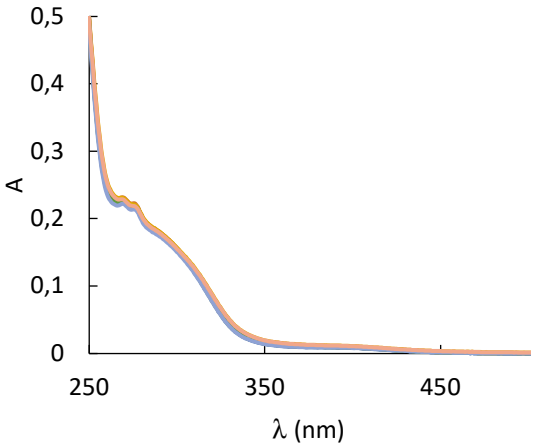

(A)

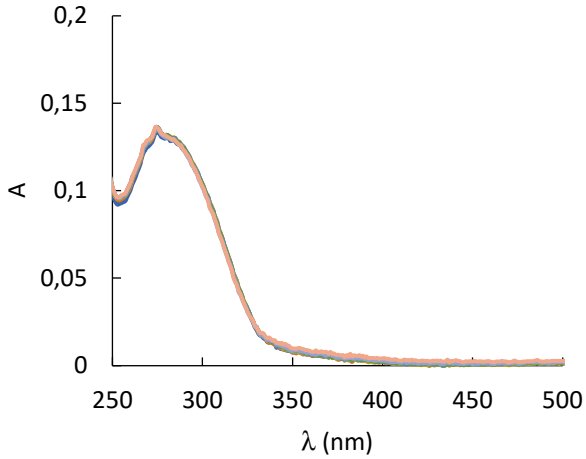

(B)

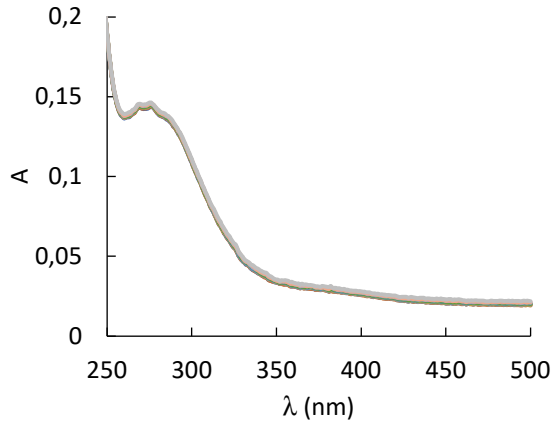

(C)

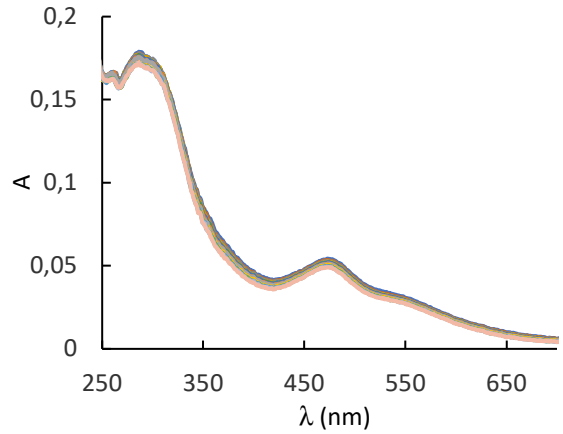

(D)

Figure S58. Time dependent UV-vis spectra (recorded every 15 minutes, 2 h 15 min total) of **7** (3.53×10^{-5} M) or **8** (3.63×10^{-5} M), 0.01 M NaCac, pH = 7.0, T = 25.0 °C. (A) – (B) – (C) – (D) **7** at 0, 0.01, 0.1 and 3 M NaCl, respectively. (E) – (F) – (G) – (H) **8** at 0, 0.01, 0.1 M and 3 M NaCl, respectively.

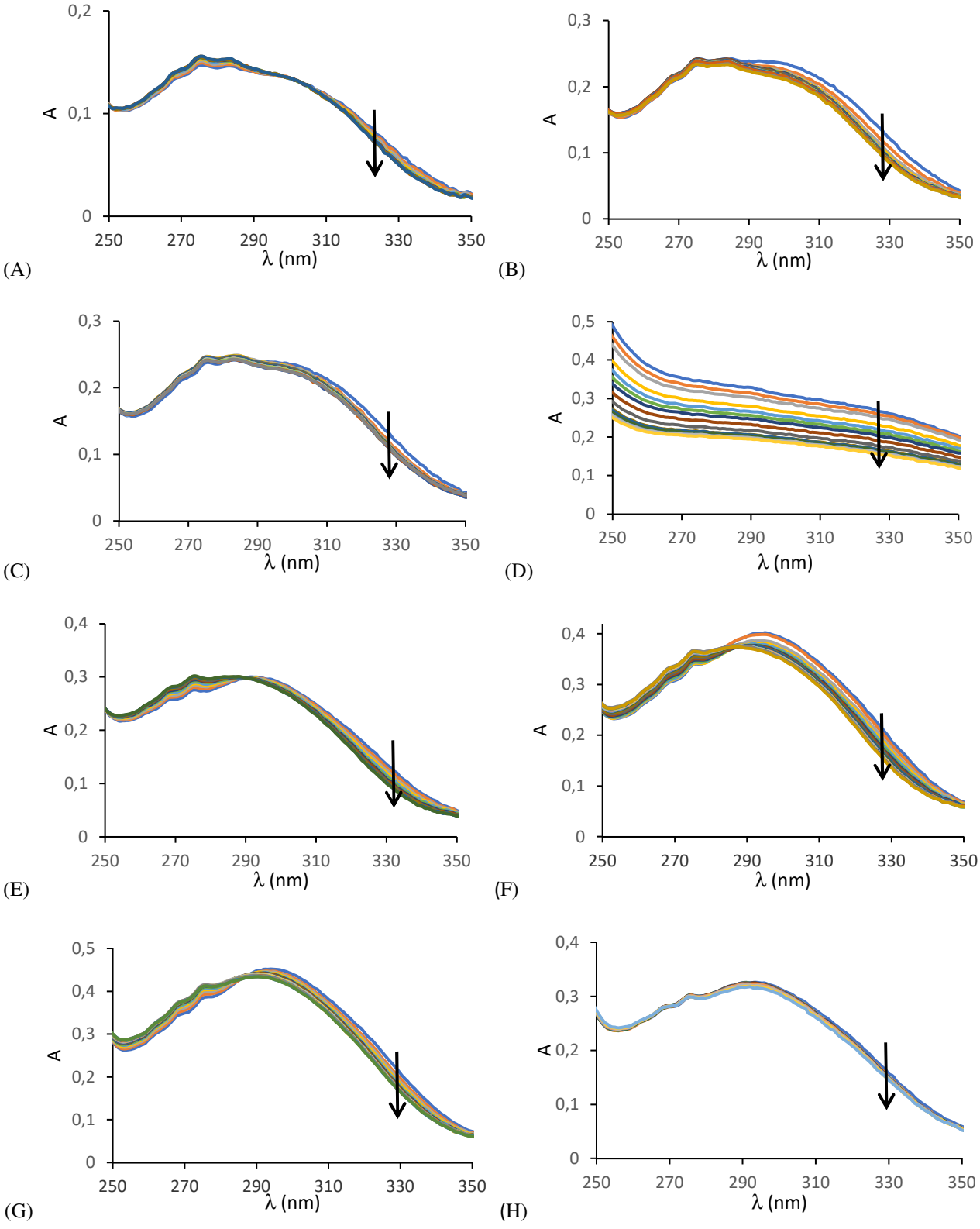

Figure S59. Absorbance vs. concentration plots of selected Ru^{II} complexes: (A) **1**, **2** and **3**; (B) $\mathbf{7}^{W}$, $\mathbf{8}^{W}$ and **13**. Conditions: 0.01 M NaCac, 0.01 M NaCl, pH = 7.0, T = 25.0 °C.

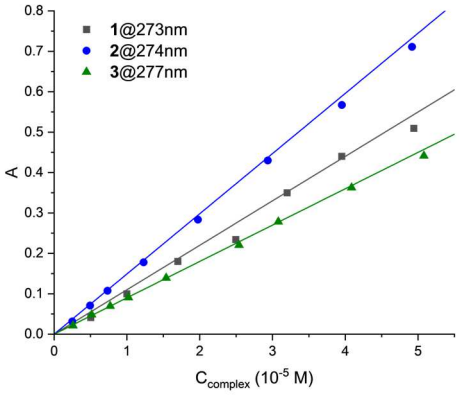

(A)

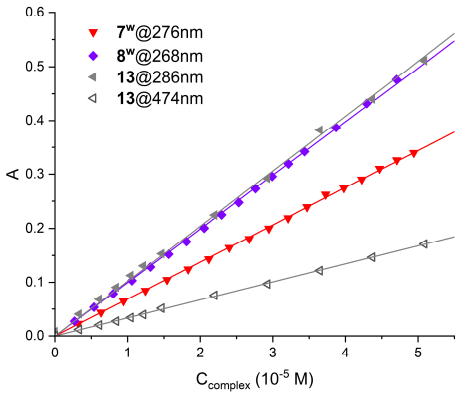

(B)

Figure S60. Representative spectrofluorimetric titration where increasing amounts of the Ru^{II} complex **8** is added to BSA: (A) emission spectra quenching; (B) relevant binding isotherm. In these experiments, the emission decrease is corrected for dilution and inner filter effects (if any). Conditions: $C_{BSA} = 9.3\times10^{-7}$ M, C_8 from 0 to 4.0×10^{-6} M, 0.1 M NaCl, 0.01 M NaCac, pH = 7.0, T = 25.0 °C.

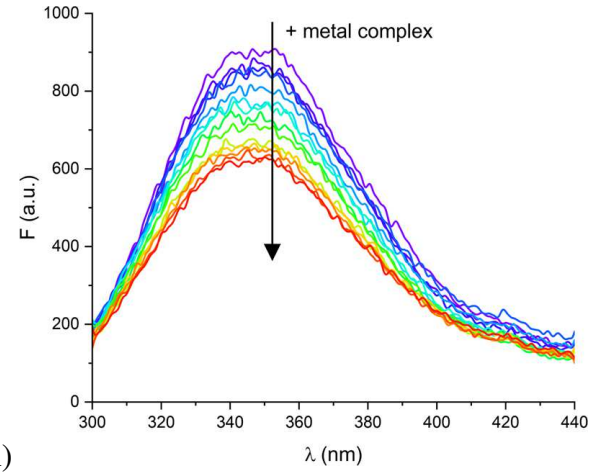

(A)

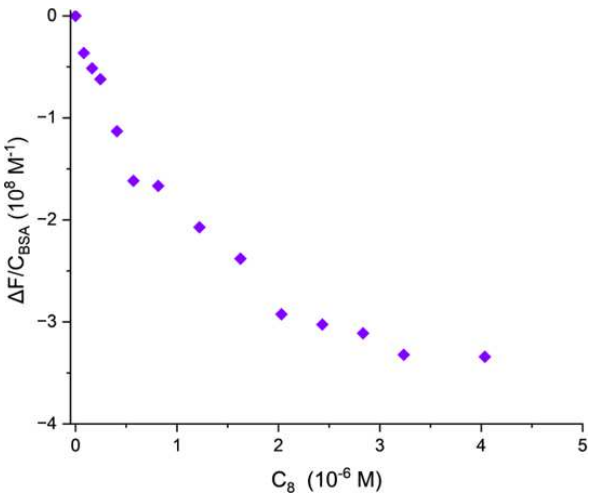

(B)

Figure S61. BSA data treatment for Ru^{II} complexes tested according to (A) modified Stern-Volmr equation and (B) binding sites equation (see Table S5 and its footnote). Note that in (B) the slope is very similar in all cases (n = 1) whereas the intercept (1/Kn) is different and much lower for the amine complexes (higher K); the inset enlarges this latter part of the overall plot. Conditions: 0.1 M NaCl, 0.01 M NaCac, pH = 7.0, T = 25.0 °C.

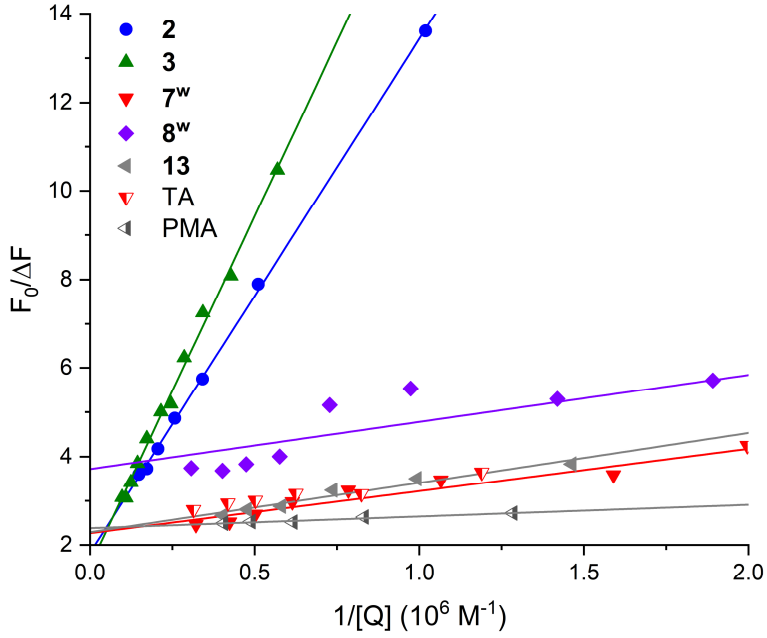

(A)

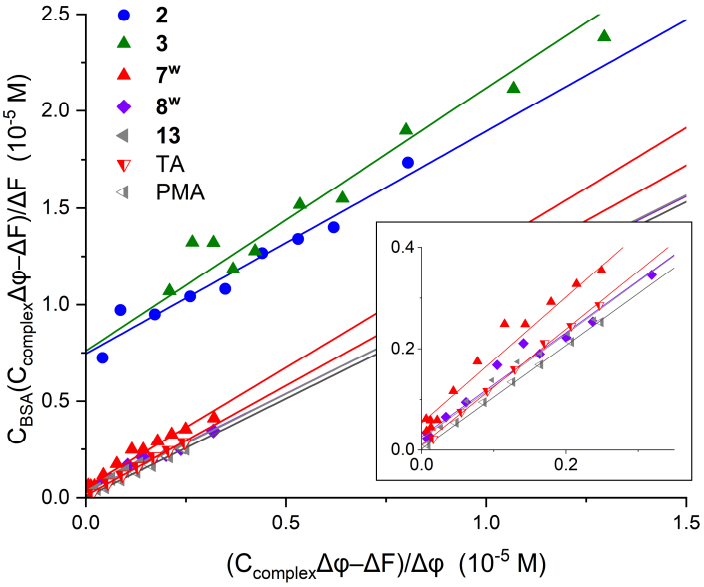

(B)

Table S7. Parameters for the binding of the Ru^{II} complexes to BSA: (i) Stern Volmer parameters (K_{SV}, f_a) from the experimental data fitting according to the modified Stern-Volmer equation (see below); (ii) complex formation stoichiometry (n) obtained according to a modified Scatchard Equation (see below); (iii) binding constants (K_{BSA}) from the HypSPec2014 software for an interaction assuming 1:1 stoichiometry. Conditions: NaCl 0.1M, NaCac 0.01 mM, pH = 7.0, T = 25.0 °C.

	2	**3**	**7^w**	**8^w**	**13**	**TA**	**PMA**
K_{SV} (10^6 M^{-1})	0.11 ± 0.02	0.12 ± 0.02	3 ± 1	3 ± 1	2 ± 1	3 ± 1	10 ± 1
f_a	0.5 ± 0.1	0.7 ± 0.1	0.4 ± 0.1	0.3 ± 0.1	0.4 ± 0.1	0.4 ± 0.1	0.4 ± 0.1
n	0.9 ± 0.4	0.8 ± 0.1	0.8 ± 0.1	0.8 ± 0.1	1.0 ± 0.1	0.9 ± 0.1	1.0 ± 0.1
K_{BSA} (10^6 M^{-1})	0.16 ± 0.06	0.14 ± 0.03	3.7 ± 0.2	2.3 ± 0.1	3.1± 0.2	2.4 ± 0.2	46 ± 7

The modified Stern-Volmer equation reads

$$\frac{F_0}{\Delta F} = \frac{1}{f_a K_{SV}[Q]} + \frac{1}{f_a}$$

where F_0 is the initial fluorescence of BSA alone, $\Delta F = F_0 - F$ where F is the fluorescence read (dilution corrected) at each addition of quencher (Q), [Q] is the concentration of free quencher in the system, K_{SV} is the Stern-Volmer constant for the quenching process, and f_a is the fraction of fluorescence accessible to the quencher. Note that, in the absence of quencher excess, $[Q] = C_Q - [Q]_{bound}$ is not known and needs to be calculated iteratively: (a) in the first step the plot is obtained assuming $[Q] = C_Q$ (with C_Q total analytical concentration of the quencher); (b) a first estimate of K_{SV} is obtained from the plot, $K_{SV} = [Q]_{bound}/([Q][P])$ where [P] is the unbound fraction of the protein $[P] = C_{BSA} - [Q]_{bound}$; (c) [Q] can be calculated at each point of the titration from K_{SV}, C_Q and C_{BSA} and a new plot is produced; (d) better K_{SV} (and f_a) estimates are obtained so to go back to step (c). The procedure is iterated until convergence.

For the numerical evaluation of the number of binding sites n (and in principle of the binding constant K), the following equation can be used, which is another form of the known Scatchard equation.

$$C_{BSA}(C_T\Delta\varphi - \Delta F)/\Delta F = (1/nK) + (C_T\Delta\varphi - \Delta F)/n\Delta\varphi$$

Here C_{BSA} is the total molar concentration of protein, C_T is the total molar concentration of the target molecule, $\Delta F = F - F_0$ and $\Delta\varphi$ represents the difference between the fluorescence coefficient of the T-BSA adduct and BSA ($\Delta\varphi = \varphi_{T\text{-}BSA} - \varphi_T$). If the direct proportionality between F and concentration holds, we can write $F = \varphi_i[i]$. This equation is analogous in fluorescence of Lambert & Beer's law: [i] is the molar concentration of the emitting species, and φ_i is an optical constant which contains the quantum yield, the molar extinction coefficient at λ_{ex}, the intensity of the exciting light beam and an instrumental factor. Therefore, $\Delta\varphi$ would be related to the changes in the optical parameters upon binding and can be calculated to the point at zero and "infinite" addition. This type of treatment mainly yields n, given that the high value of K would reflect in an intercept that is too low to be used robustly.